Supporting Information

Twist and Charge Transfer Modulation in Imidazo[1,2-a]pyridine encapped 1,3,5-Triazine Towards Multifunctional Green-Emissive DSEgens: Applications in TNP Sensing, Bioimaging, and Organic Light Emitting Diodes

Chinmay Thakkar, [a] Mohammad Amir Ahemad, [b] Shweta Nikumbh, [b] Monalisha Debnath, [c] Ketaki Kadam, [a] Mahesh Dhere, [a] Anjali Tripathi, [d] Dr. Purav Badani, [d] Rohit Srivastava, [c] Dr. Sangita Bose[b] and Dr. Satyajit Saha[a]**

[a]Department of Speciality Chemicals Technology, Institute of Chemical Technology (ICT), Mumbai, Maharashtra-400019, India
[b]Department of Physics, UM-DAE Centre for Excellence in Basic Sciences, Mumbai, Maharashtra, India
[c]Department of Biosciences and Bioengineering, Indian Institute of Technology Bombay, Mumbai, Maharashtra, India
[d]Department of Chemistry, University of Mumbai, Kalina Campus, Mumbai, Maharashtra, India
Corresponding authors E-mail: ss.saha@ictmumbai.edu.in (SS), sangita@cbs.ac.in (SB)

Table of Contents

General aspects:

Chemicals: All target molecules were synthesised via name reactions like Grindstone Chemistry, Heck reaction, Friedel Craft acylation, Ullman reactions. Chemicals required were purchased from commercial sources like Sigma-Aldrich, Spectrochem, S. D. Fine chemicals, BLDpharma, Avra, Oxford and used without further purification.

Thin Layer Chromatography (TLC): Reaction completion was monitored via Thin Layer Chromatography (TLC) using Silica gel-coated aluminium sheets (ACME, 254F) with Ethyl Acetate, Petroleum Ether as eluents.

Fourier Transform Infrared (FTIR): Product analysis carried out using Fourier transform infrared (FTIR) (ATR-IR) spectra which is obtained with Alpha-II/Bruker-instrument.

Nuclear Magnetic Resonance (NMR): ^{1}H Nuclear Magnetic Resonance (^{1}H NMR) spectroscopy was carried out on Bruker 400 and 500 MHz spectrometer whereas ^{13}C NMR was carried out on 100 MHz spectrometer using $CDCl_3$ as a solvent. Chemical shifts were reported in parts per million (ppm) downfield from TMS, and the spin multiplicities are described as s (singlet), d (doublet), t (triplet), and multiplet (m). Coupling constant (J) values are reported in hertz (Hz).

Thermogravimetric analysis (TGA): Thermogravimetric analysis (TGA) was conducted on a Perkin-Elmer Diamond TG/DTA instrument at a heating rate of 10 °C/min under a nitrogen atmosphere with a 150 mL/min flow rate.

UV-Visible Spectrophotometer (UV-Vis): Absorption spectra were obtained on a FP-8200/Jasco spectrophotometer. And

Spectrofluorimeter: Emission spectra (liquids) and Solid-state emission was obtained on FP-8200/Jasco spectrofluorimeter.

Cyclic voltammeter (CV): Redox potential is determined using PS-091 Cyclic voltammeter (Admiral Instruments) using 0.1M solution of tetrabutylammonium hexafluorophosphate ($^tBu_4NPF_6$) in tetrahydrofuran (0.1 M) as an electrolyte, platinum gauze and Ag/AgCl as a counter and reference electrodes respectively with a scan rate of 20 mV/s.

Density Functional Theory (DFT): DFT studies of luminogens obtained via B3LYP functional with basis set 6-311++ G (d, p) using the Gaussian16 programme.

Time-Correlated Single Photon Counting (TSCPC): Time-resolved fluorescence measurements were measured using a time-correlated single photon counting (TCSPC) unit (Horiba Deltaflex). The laser used for all the samples was of 510 nm. All the measurements were undergone at room temperature. The decay fitting was done by keeping the χ^2 value close to 1.

Thermally Activated Delayed Fluorescence Quantum Yield Experiments: Phosphorescence lifetime, gated emission and time-resolved excitation and emission were measured on FLS1000 spectrometer, Edinburgh Instruments equipped with a micro flash-lamp (µF2) set-up. Fluorescence lifetimes were performed on the same instrument. A 405 nm laser diode with a pulse repetition rate of 20 MHz were used as the light sources. Quantum yields were measured using an integrating sphere in the same instrument.

Dynamic Light Scattering (DLS): Dynamic Light Scattering studies were performed to measure partial size distribution in solutions by analysing the fluctuations in scattered light caused by Brownian motion. Studies perform on Malvern Zetasizer Nano-ZS90 instrument using sample evolving aggregates in THF at high water fraction.

Bioimaging Studies: Dulbecco's modified eagle's media (DMEM), trypsin-EDTA solution (0.25% trypsin and 0.02% EDTA in DPBS), fetal bovine serum (FBS), dulbecco's phosphate-buffer saline (DPBS), and antibiotic antimycotic solution (10000 units of penicillin, 10.0 mg of streptomycin, and 25 µg of amphotericin B per mL in 0.9% normal saline), dimethyl sulfoxide (DMSO) (≥99.5%), trypan blue, 3-(4,5-dimethylthiazol-2-yl)-2,5-diphenyl tetrazolium bromide (MTT), and tetrahydrofuran (THF), and 37% formaldehyde solution were purchased from HiMedia Laboratories Pvt. Ltd. 4´, 6-diamidino-2-phenylindole (DAPI) was procured from Merck Ltd., India. 2´, 7´-dichlorofluorescin diacetate (DCFDA), 30% hydrogen peroxide were supplied by Sigma Aldrich.

Cells and culture conditions: Human embryonic kidney cell lines (HEK-293) and cervical cancer cell lines (HeLa) were procured from NCCS, Pune, India. The cells were cultured with complete DMEM (DMEM supplemented with 10% v/v FBS and 1% v/v antibiotic antimycotic solution), and the incubation conditions were 37°C and 5% CO_2.

Synthetic Procedures and Characterization Data of 6,8 and 10.

Intermediates 6, and 8 were synthesized using previously reported synthetic procedure 6[1], 8[2]:

Synthesis of 3,6-di-tert-butyl-9-(4-(imidazo[1,2-a]pyridin-2-yl)phenyl)-9H-carbazole (10): In a dry 50 ml pressure vessel equipped with a magnetic stirre, a mixture of aryl halide **8** (2.5 g, 9.153 mmol), 3,6-di-tert-butyl-9H-carbazole **9** (3.06 g, 10.98 mmol), CuI (0.52 g, 0.3 mmol), 1,10-phenanthroline (0.49 g, 0.3 mmol) as ligand, and K_2CO_3 (3.16 g, 22.88 mmol) as base was added under a nitrogen atmosphere. Anhydrous DMF (20 mL) was added as solvent, and the reaction mixture was stirred at 145 °C for 72 h. After cooling it to room temperature the mixture was poured into ice cold water (50 mL), and extracted with DCM (3 × 20 mL). The combined organic layers were washed with brine, dried over anhydrous Na_2SO_4, filtered, and concentrated under reduced pressure. The crude product was purified by column chromatography on silica gel using hexane/ethyl acetate as eluent to afford 1.95 g of 3,6-di-tert-butyl-9-(4-(imidazo[1,2-a]pyridin-2-yl)phenyl)-9H-carbazole **10** the desired product. Yield = 45%. R_f = 0.25 (75:25 Petroleum Ether:EtOAc). ^{1}H NMR (500 MHz, $CDCl_3$): δ 8.22 – 8.07 (m, 5H), 7.93 (d, *J* = 4.3 Hz, 1H), 7.70 – 7.60 (m, 3H), 7.45 (dt, *J* = 12.4, 6.7 Hz, 4H), 7.24 – 7.16 (m, 1H), 6.81 (dd, *J* = 12.1, 5.3 Hz, 1H), 1.47 (d, *J* = 4.2 Hz, 18H); ^{13}C NMR (126 MHz, $CDCl_3$): δ 144.8, 144.0, 141.9, 138.1, 136.8, 131.3, 126.3, 125.9, 124.6, 122.6, 122.3, 116.6, 115.2, 111.6, 108.3, 107.2, 33.7, 31.0.

Synthesis of 2,4,6-tris(4-(2-(4-(3,6-di-tert-butyl-9H-carbazol-9-yl)phenyl)imidazo[1,2-a]pyridin-3-yl)phenyl)-1,3,5-triazine (ANU-1): In a 25 ml pressure tube, charged with a magnetic stir bar, 10 ml of *N, N* –dimethylacetamide was added with nitrogen purging followed by the addition of **12** (0.18 g, 0.33 mmol), **10** (0.52 g, 1.11 mmol), pivalic acid (0.062 g, 0.60 mmol), PCy_3HBF_4 (0.037 g, 0.10 mmol), $Pd(OAc)_2$ (0.009 g, 0.04 mmol) and K_2CO_3 (0.16 g, 1.182 mmol). After the addition, the tube was purged with nitrogen, sealed, and heated at 120 ℃ for 48 hours. The reaction mixture was cooled to room temperature, poured into ice-cold water, and extracted with DCM. The organic phase was dried over Na_2SO_4. The evaporation of the organic solvent gave a crude product which was further purified, with column chromatography using *n*-hexane and ethyl acetate as eluent. After purification, 0.36 g of 2,4,6-tris(4-(2-(4-(3,6-di-tert-butyl-9H-carbazol-9-yl)phenyl)imidazo[1,2-a]pyridin-3-yl)phenyl)-1,3,5-triazine **ANU-1** was obtained in 64% yield; R_f = 0.6 (50:50 Petroleum Ether:EtOAc); Melting point: 264°C; IR (cm^{-1}): 739, 810, 1024, 1239, 1357, 1512, 2952; ^{1}H NMR (500 MHz, $CDCl_3$): δ 9.07 – 9.00 (d, 6H), 8.15-8.16 (d, 3H), 8.10 (s, 6H), 7.92-7.94 (d, 6H), 7.83-7.81 (d, *J* = 8.1 Hz, 6H), 7.78-7.76 (d, *J* = 9.0 Hz, 3H), 7.53-7.51 (d, *J* = 8.3 Hz, 6H), 7.43 – 7.38 (m, 13H), 7.32 – 7.29 (t, 3H), 6.86 – 6.83 (t, 3H), 1.42 (s, 54H); ^{13}C NMR (126 MHz, $CDCl_3$): δ 171.4, 145.4, 142.9, 142.5, 139.0, 137.7, 136.3, 134.3, 132.5, 130.9, 130.3, 129.5, 126.5, 125.4, 123.6, 123.4, 120.5, 117.9, 116.2, 112.9, 109.3, 34.7, 31.9; HRMS: Calcd. for $C_{120}H_{108}N_4$ (M^++H)+: 1718.8736; found: 1718.8976.

Synthesis of 2,4,6-tris(4-(2-(4-(1,2,2-triphenylvinyl)phenyl)imidazo[1,2-a]pyridin-3-yl)phenyl)-1,3,5-triazine (ANU-2): In a 25 ml pressure tube, charged with a magnetic stir bar, 10 ml of *N, N*–dimethylacetamide was added with nitrogen purging followed by the addition of **12** (0.2 g, 0.37 mmol), **6** (0.57 g, 1.20 mmol), pivalic acid (0.067 g, 0.66 mmol), PCy_3HBF_4 (0.04 g, 0.10 mmol), $Pd(OAc)_2$ (0.01 g, 0.04 mmol) and K_2CO_3 (0.18 g, 1.28 mmol). After the addition, the tube was purged with nitrogen, sealed, and heated at 120 ℃ for 48 hours. The reaction mixture was cooled to room temperature, poured into ice-cold water, and extracted with DCM. The organic phase was dried over Na_2SO_4. The evaporation of the organic solvent gave a crude product which was further purified, with column chromatography using *n*-hexane and ethyl acetate as eluent. After purification, 0.42 g of 2,4,6-tris(4-(2-(4-(1,2,2-triphenylvinyl)phenyl)imidazo[1,2-a]pyridin-3-yl)phenyl)-1,3,5-triazine **ANU-2** was obtained in 70% yield; R_f = 0.5 (50:50 Petroleum Ether:EtOAc); Melting point: 282°C; IR (cm^{-1}): 745, 819, 1354, 1501, 1598, 2352; ^1H NMR (500 MHz, $CDCl_3$): δ 8.95 (d, *J* = 8.3 Hz, 6H), 8.12 (d, *J* = 6.9 Hz, 3H), 7.69 (dd, *J* = 8.7, 4.4 Hz, 9H), 7.45 (d, *J* = 8.3 Hz, 6H), 7.24 (d, *J* = 8.1 Hz, 2H), 7.11 – 7.01 (m, 40H), 6.98 (dd, *J* = 8.4, 5.1 Hz, 12H), 6.80 (t, *J* = 6.5 Hz, 3H); ^{13}C NMR (126 MHz, $CDCl_3$): δ 171.3, 145.3, 143.6, 143.5, 143.3, 143.2, 141.2, 140.6, 136.0, 134.4, 132.9, 131.5, 131.4, 131.3, 131.3, 130.7, 130.0, 127.7, 127.6, 127.5, 126.4, 120.3, 117.7; HRMS: Calcd. for $C_{120}H_{81}N_9$ $(M^++H)+$: 1649.6771; found: 1649.6646.

Differential Scanning Calorimetry Data for ANU-1 and ANU-2

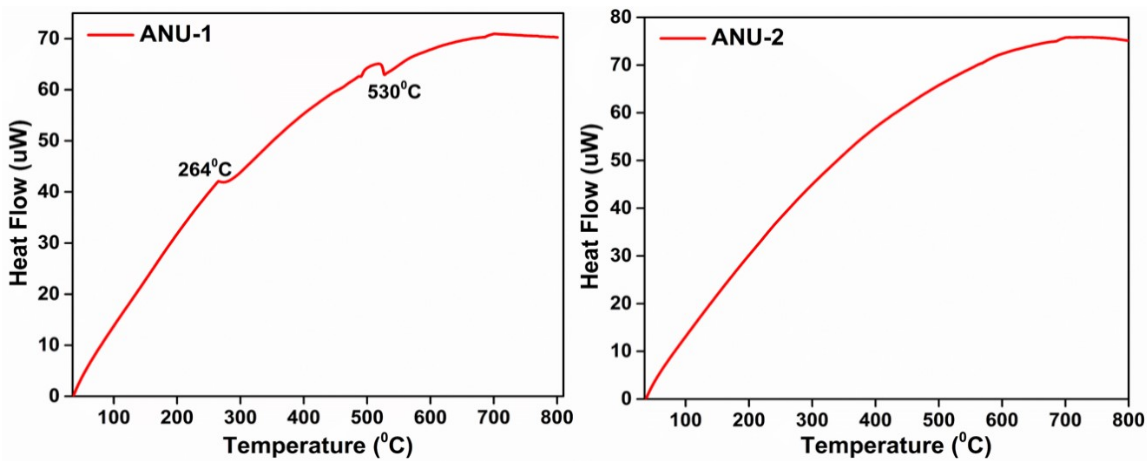

Figure S1. DSC profiles of **ANU-1** and **ANU-2**.

Photophysical Studies of ANU-1 and ANU-2

Preparation of stock solution luminogen ANU-1 in THF solvent
Molecular weight = 1718.17 g
Therefore, 17.18 g in 1000 mL of THF ≡ 1M

$$Concentration\ (M) = (Mass\ (g))/(Formula\ weight\ (g) * Volume\ (L))$$

Hence, to prepare 1mM stock solution 17.18 mg of **ANU-1** was dissolved in 10 ml THF
Similarly stock solutions of **ANU-2** were prepared.

Solvatochromism studies of ANU-1 and ANU-2

To investigate the behavior of the luminogens in the presence of different solvents with graded polarity solvatochromism study was carried out where among the synthesized luminogens some are emissive in THF, so variation in this luminogens absorption or emission properties in different solvents was measured.

Table S1. Absorption, Emission of **ANU-1** and **ANU-2** in solvents of various polarity.

Solvents	Compounds			
	ANU-1		ANU-2	
	λ_{abs} (nm)	λ_{em} (nm)	λ_{abs} (nm)	λ_{em} (nm)
***n*-hexane**	342,398	470	338,409	463
Toluene	343,399	482	342,411	473
Chloroform	343,398	518	339,401	491
Acetone	340,393	528	339,403	516
Methanol	339,392	529	332,395	512
ACN	340,393	535	332,403	523
DMSO	340,392	537	338,404	530
DMF	340,393	538	338,406	529

Fluorescence Quantum Yield Calculation of ANU-1 and ANU-2 (Relative Method)

The fluorescence quantum yield of **SK-1** to **SK-6** was measured in different solvents in which they show Solvatochromism with respect to quinine sulphate which was taken as a standard (Φ = 0.54 in 0.1 M H_2SO_4).

$\varphi\_x = \varphi\_ST * ((⟦Grad⟧\_x))/((⟦Grad⟧\_ST)) * ⟦(\eta\_x)⟧^2/⟦(\eta\_ST)⟧^2$

Here, ϕ_x = Quantum yield (**ANU-1 to ANU-2**)

ϕ_{ST} = Quantum yield (quinine sulphate)

η_x = Refractive index of different solvents

η_{ST} = Refractive index of 0.1M H_2SO_4

In order to find out gradient for all this molecules, optical density (from UV) vs curve area (from emission) in solvent was plotted. The absorption and emission wavelength of all luminogens were recorded in different solvents by keeping the absorption maxima to be < 0.1. Slowly concentration decreases by performing 50% dilution and readings were taken until it reaches to 0. The same followed for 0.1M quinin sulphate, which was diluted by 0.1M H_2SO_4. All values were recorded in UV-vis spectrophotometer and summarized in Table S2.

Table S2. Quantum Yield (relative method) data of **ANU-1** and **ANU-2** in solvents of various polarity.

Solvents	Compounds	
	ANU-1 **Ø PL (%)**	**ANU-2** **Ø PL (%)**
***n*-hexane**	3.02	5.55
Toluene	8.28	10.52
Chloroform	43.20	17.68
Acetone	9.65	11.05
Methanol	--	--
ACN	5.80	8.33
DMSO	6.01	0.94
DMF	2.8	3.28

--- = not emissive enough to calculate quantum yield

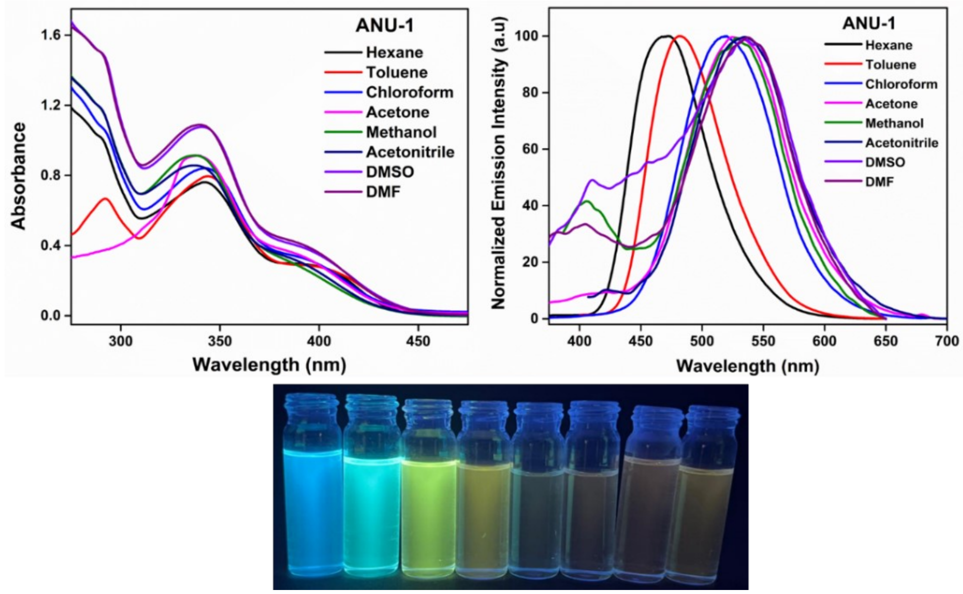

Figure S2. Absorption, emission spectra of **ANU-1** with photo of solvent vials arranged according to polarity ratio (From left: *n*-hexane, Toluene, Chloroform, Acetone, Methanol, Acetonitrile, DMSO, DMF).

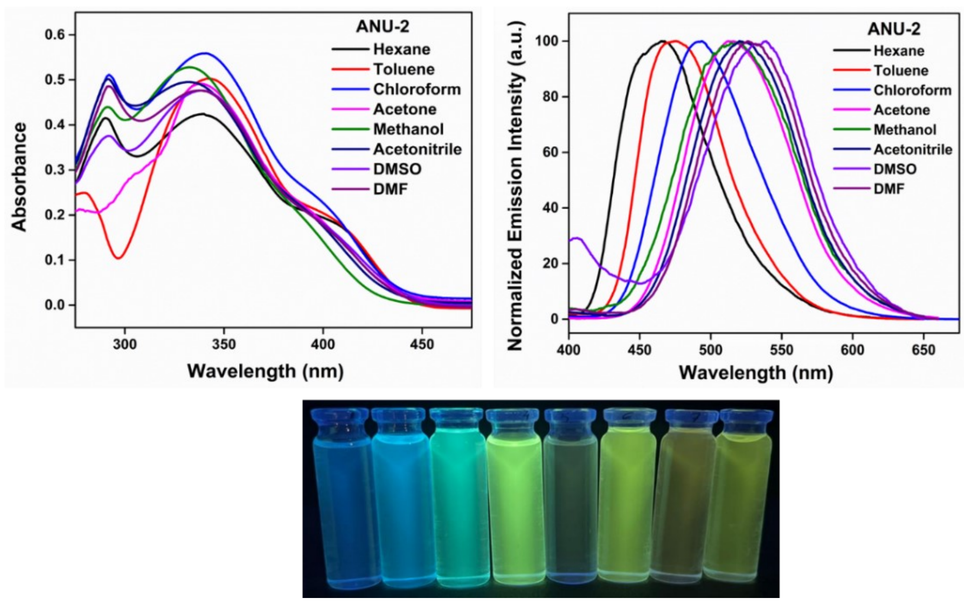

Figure S3. Absorption, emission spectra of **ANU-1** with photo of solvent vials arranged according to polarity ratio (From left: *n*-hexane, Toluene, Chloroform, Acetone, Methanol, Acetonitrile, DMSO, DMF).

Aggregation Induced Emission Studies of ANU-1 and ANU-2

Aggregation-induced emission (AIE) studies were conducted to elucidate the photophysical properties of molecules in suitable solvent of different concentrations with water under varying aggregation and dilution states. All studies were performed using tetrahydrofuran in different concentration with water. The concentration of stock solution of **ANU-1** and **ANU-2** used for studied was 1 mM. Absorption studies performed in JASCO V-750 spectrophotometer under room temperature using two side opaque and two side transparent quartz cuvettes having path length equalled to 1 cm. For photoluminescence studies, the emission measurement was performed in a JASCO FP-8200 spectrofluorometer under room temperature using all side transparent quartz cuvette with path length equal to 1cm.

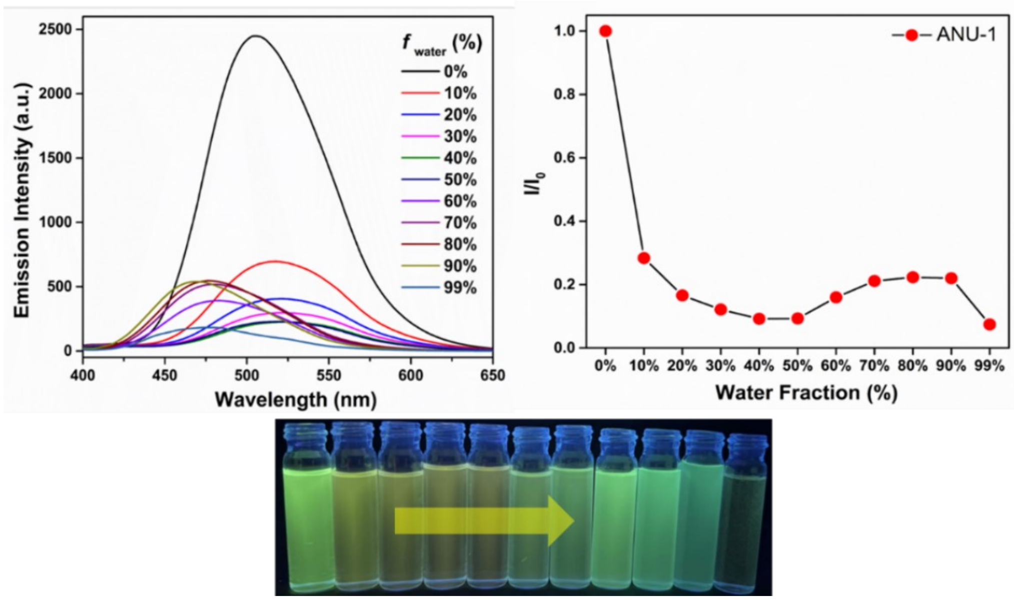

Figure S4. a) AIE emission, b) I/I_0 graph of **ANU-1** and c) vials showing AIE solutions of **ANU-1** (left to right: 0% water to 99% water).

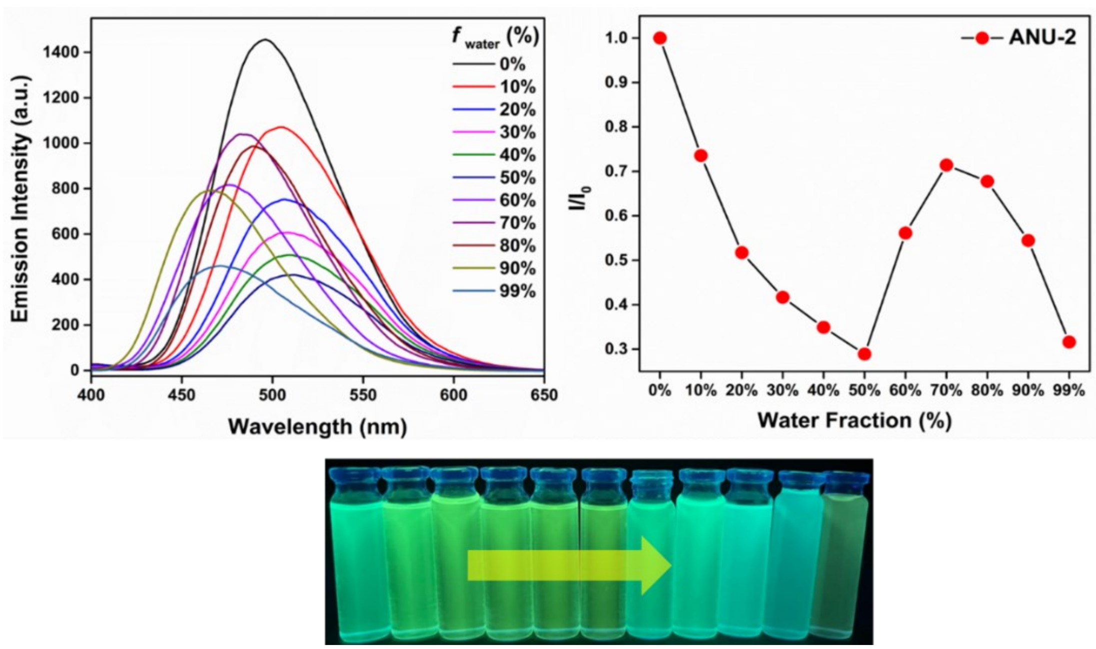

Figure S5. a) AIE emission, b) I/I_0 graph of **ANU-2** and c) vials showing AIE solutions of **ANU-2** (left to right: 0% water to 99% water).

Dynamic Light Scattering (DLS) Experiments and Tyndall Effect of ANU-2.

The size distribution of the evolved aggregates in THF at higher water fraction was determined through a DLS experiment, using the Malvern Zetasizer Nano-ZS90 instrument. A transparent disposable polystyrene cuvette with a path length equal to 1 cm, containing the desired solution was utilized in the experiment. A 632.8 nm red laser was employed as an excitation source at a fixed scattering angle (90˚ optics). Tyndall effect was studied by passing laser light through the maximum aggregated state and dilution state (100% THF) of luminogens. The solution containing 99% water shows light scattering and make the beam visible which confirms aggregate formation. While in 100% THF solution light pass away without any appearance, that indicates that no aggregates have been formed. **ANU-2** showed presence of aggregates in 70% Water:THF medium with the average aggregate size of 656.67 nm.

Computational Details of ANU-1 and ANU-2.

In our current study, we focused on the geometry optimization of a given structure using the Gaussian 09 program. To achieve this, we employed the Density Functional Theory (DFT) approach, specifically utilizing the B3LYP functional and the 6-311G basis set. Furthermore, in order to refine the energy, we performed single-point energy calculations at the B3LYP/6-311++G(d,p) level of theory. In addition to optimizing the structure and refining the energy calculations, we also investigated the impact of the solvent on the structures. To achieve this, we conducted single-point electronic structure calculations using an implicit CPCM model at the B3LYP/6-311++G(d,p) level of theory. Specifically, we considered the THF (tetrahydrofuran) solvent environment respectively. The Cartesian coordinates for the optimized structure is provided.

ANU-1

Total energy: -5294.79385627 a.u.

Charge: 0

Spin: Singlet

Dipole moment: 5.2700 Debye

Function/Basis set: B3LYP/6-311G

N	-0.82641600	0.37005900	-3.88738000
C	-0.43416700	-0.74235700	-3.21965800
N	0.76335200	-0.84690700	-2.59440800
C	1.58623700	0.22817400	-2.66130500
N	1.26314600	1.36662700	-3.32183800
C	0.04856500	1.40483600	-3.92116200
C	-0.33994100	2.62980100	-4.64112600
C	-1.35289900	-1.89264200	-3.17084700
C	2.88768300	0.15985500	-1.97608900
C	3.24519200	-0.97827500	-1.23413200
C	4.46693600	-1.03395600	-0.57084100
C	5.37415900	0.04311700	-0.63161700
C	5.01202200	1.17668400	-1.38510800

C	3.78804900	1.23722000	-2.04152300
C	-1.60013300	2.72881400	-5.25406800
C	-1.96687700	3.88776800	-5.93100100
C	-1.08711800	4.98523400	-6.01793900
C	0.17423600	4.87833100	-5.40129500
C	0.54297400	3.71995600	-4.72593200
C	-2.62136400	-1.81991900	-3.76991400
C	-3.49004900	-2.90554200	-3.71847900
C	-3.11817100	-4.10205200	-3.07266500
C	-1.84258700	-4.16859300	-2.47913500
C	-0.97698200	-3.08149500	-2.52230000
C	-4.02814300	-5.25578900	-3.01967500
C	6.66542900	-0.00474900	0.06982400
C	-1.47393800	6.21745500	-6.72281300
C	-0.90019800	6.93062700	-7.78421000
N	-1.61920100	8.08592700	-8.04787100
C	-2.63758800	8.11036200	-7.18028100
N	-2.59496600	6.96840200	-6.34044900
C	0.26558300	6.60914100	-8.61778300
C	0.89064100	7.64506000	-9.33719500
C	1.98764900	7.39024500	-10.15388900
C	2.47797600	6.08421000	-10.29343200
C	1.85326400	5.04183200	-9.59637900
C	0.76583900	5.30290800	-8.76537500
C	7.27672600	0.85154700	0.99690200
N	8.54551700	0.40054200	1.32289700
C	8.74280600	-0.72591900	0.62782800

N	7.60191300	-1.02320000	-0.16057500
C	6.76119800	2.06623700	1.64325900
C	7.67698200	2.98389600	2.19165900
C	7.23907100	4.14092900	2.82865500
C	5.86849400	4.41851800	2.92751600
C	4.94692400	3.50683600	2.39641800
C	5.38811900	2.34132400	1.77349200
C	-4.52334900	-6.03204400	-1.96190500
N	-5.31305800	-7.06658900	-2.43724300
C	-5.33231200	-6.95387700	-3.77049000
N	-4.55419700	-5.84154300	-4.18086200
C	-4.34516500	-5.87842500	-0.51144300
C	-4.57255700	-6.99095100	0.32067700
C	-4.43388100	-6.89405100	1.70170000
C	-4.05348700	-5.68036400	2.29150400
C	-3.83520500	-4.56318200	1.47491800
C	-3.99109600	-4.65923700	0.09357900
C	-5.96665800	-7.73837700	-4.75819800
C	-5.80265800	-7.42045100	-6.08539500
C	-4.98958500	-6.31135800	-6.46434400
C	-4.37409300	-5.53991400	-5.51814200
C	9.85326600	-1.59547100	0.56714900
C	9.81149000	-2.69219400	-0.26045400
C	8.65835000	-2.94612100	-1.06082000
C	7.57402600	-2.11501300	-1.00834100
C	-3.67375800	9.05074300	-6.99195300
C	-4.60084900	8.84812700	-5.99752300

C	-4.51308100	7.70089400	-5.15426700
C	-3.51750100	6.78004900	-5.32801400
N	3.58898900	5.81795900	-11.14517800
C	3.68287300	6.15731900	-12.51050500
C	4.93501300	5.72257900	-13.00988400
C	5.63708800	5.09211400	-11.90544500
C	4.78232300	5.16612100	-10.77381300
C	2.75546900	6.77959500	-13.34931800
C	3.10789100	6.97396600	-14.68266500
C	4.35520500	6.56387600	-15.21568700
C	5.26082700	5.93160500	-14.35662400
C	6.89586900	4.49838800	-11.78393700
C	7.32723300	3.97820300	-10.55388200
C	6.45489100	4.08117600	-9.44758500
C	5.19058400	4.66915400	-9.53748400
N	-3.89550700	-5.58276800	3.70446200
N	5.41660900	5.61165600	3.56265300
C	-4.53697500	-4.65412400	4.54891800
C	-4.11256400	-4.87443700	5.88269700
C	-3.17314000	-5.98082100	5.85233200
C	-3.06320900	-6.39442600	4.50163900
C	4.49062600	5.68768100	4.62274600
C	4.27941000	7.04921600	4.95315200
C	5.10815500	7.83696100	4.05886600
C	5.79498000	6.92552400	3.21916100
C	3.85173000	4.67100600	5.33682800
C	2.98972500	5.03837400	6.36709400

C	2.74260200	6.38937100	6.71733900
C	3.40578200	7.38754000	5.99553200
C	-5.47816100	-3.66548000	4.25183800
C	-5.96919700	-2.89403900	5.30208700
C	-5.55914000	-3.07610500	6.64654400
C	-4.62594400	-4.08211900	6.91871300
C	-2.42276900	-6.62746500	6.84393100
C	-1.56190300	-7.67835300	6.50974700
C	-1.47089200	-8.05709100	5.14704700
C	-2.20216300	-7.43307000	4.13936600
C	8.72488300	3.32610600	-10.44849200
C	9.02305800	2.79831000	-9.02710600
C	8.81701700	2.12921700	-11.43261700
C	9.81507900	4.37004000	-10.81038500
C	4.66215100	6.82451200	-16.70674600
C	4.62380400	8.35091900	-16.98657200
C	6.05496300	6.29732400	-17.11893000
C	3.60107400	6.11574700	-17.59071900
C	1.76604800	6.70442100	7.87177900
C	2.27798800	6.05090500	9.18324400
C	1.62260900	8.22266000	8.11976900
C	0.36078600	6.13828100	7.53272800
C	-6.15363000	-2.16942900	7.74642800
C	-7.69785000	-2.32423700	7.77440000
C	-5.61370100	-2.51972400	9.15114300
C	-5.79329900	-0.68889000	7.44963500
C	-0.71761200	-8.43141300	7.56128800

C	0.78837800	-8.31919100	7.20259300
C	-0.91244000	-7.86362300	8.98499900
C	-1.12823500	-9.92841300	7.58060900
C	5.30193800	9.21578800	3.89926400
C	6.16778300	9.70134800	2.91357300
C	6.83037300	8.75970300	2.08708700
C	6.65682800	7.38420600	2.21996700
C	6.42398800	11.20911200	2.69847000
C	6.05535200	11.60235400	1.24287800
C	5.58685000	12.08813700	3.65467900
C	7.92439100	11.52047700	2.94771200
H	2.54847200	-1.80050200	-1.17456500
H	4.71026300	-1.90350900	0.02522600
H	5.69965300	2.00815600	-1.44860900
H	3.51429700	2.10968700	-2.61483600
H	-2.27345500	1.88707700	-5.19781000
H	-2.93108200	3.93843700	-6.41942900
H	0.85802500	5.71395400	-5.45252300
H	1.50854400	3.64517400	-4.24959200
H	-2.91348300	-0.90315700	-4.25907100
H	-4.47576000	-2.82044500	-4.15647500
H	-1.53752100	-5.08117000	-1.98682900
H	-0.00025000	-3.13812200	-2.06670400
H	0.49960600	8.64656200	-9.23906200
H	2.47605400	8.19972500	-10.67770700
H	2.20546100	4.02853200	-9.72789800
H	0.28631100	4.47873300	-8.25879800

H	8.73079100	2.75853300	2.12584400
H	7.95236400	4.82600200	3.26467200
H	3.88920500	3.71709700	2.46758300
H	4.65681900	1.64466800	1.39229400
H	-4.87950500	-7.91952900	-0.13655200
H	-4.63331100	-7.75027900	2.33042000
H	-3.53886200	-3.62573500	1.92372600
H	-3.83876600	-3.77802600	-0.51116200
H	-6.56260900	-8.57579000	-4.43018800
H	-6.28301400	-8.01287500	-6.85056600
H	-4.84845900	-6.07171600	-7.50741300
H	-3.74021000	-4.69955400	-5.74646700
H	10.71023900	-1.36133900	1.17935100
H	10.65462200	-3.36551400	-0.31497300
H	8.63217700	-3.79898300	-1.72208900
H	6.68296900	-2.25041000	-1.59818200
H	-3.69825700	9.91062900	-7.64312400
H	-5.39868700	9.56019900	-5.84378600
H	-5.23298400	7.55038100	-4.36406000
H	-3.39511600	5.90201800	-4.71604900
H	1.78936900	7.09737600	-12.98457700
H	2.38919100	7.45737300	-15.33044200
H	6.21947900	5.59331800	-14.72144900
H	7.54090600	4.44710300	-12.65153500
H	6.76274000	3.69850800	-8.48637000
H	4.55628200	4.73813200	-8.66539200
H	4.02201800	3.62871600	5.10837000

H	2.49608000	4.25027300	6.91955900
H	3.25717000	8.43001500	6.23578800
H	-5.82623300	-3.50346500	3.24183100
H	-6.69758200	-2.12855400	5.07077700
H	-4.29367700	-4.26373600	7.93024100
H	-2.51615600	-6.29856300	7.86839500
H	-0.80616200	-8.86280300	4.86609200
H	-2.09747300	-7.74577700	3.11036200
H	10.01709300	2.34697400	-9.00759000
H	9.00894100	3.60088100	-8.28716800
H	8.30499700	2.03462100	-8.72181800
H	9.80256500	1.66092100	-11.36861000
H	8.66192500	2.44508600	-12.46505500
H	8.06322700	1.37598200	-11.19524300
H	9.77816800	5.21924500	-10.12535700
H	10.80847500	3.91880700	-10.74512900
H	9.68522300	4.75130400	-11.82405100
H	4.83754700	8.54850400	-18.04008200
H	3.64634400	8.77642800	-16.75606900
H	5.36828500	8.87209500	-16.38170600
H	6.22350800	6.50371000	-18.17776000
H	6.13658400	5.21826600	-16.97356700
H	6.85369600	6.78313300	-16.55493300
H	2.59457600	6.48197100	-17.38429200
H	3.81166700	6.29157400	-18.64872400
H	3.60990400	5.03855700	-17.41366300
H	1.59205300	6.26727300	10.00620600

H	2.35761300	4.96716000	9.08944900
H	3.26372800	6.43861600	9.44726800
H	0.92564900	8.39351900	8.94271700
H	1.23230600	8.74001200	7.24105800
H	2.57674600	8.67764500	8.39275900
H	0.38682000	5.05720000	7.38976800
H	-0.34040300	6.35353500	8.34313500
H	-0.02505400	6.58916000	6.61634300
H	-8.12772800	-1.68648200	8.55095200
H	-8.14837300	-2.04195800	6.82198400
H	-7.97786800	-3.35804100	7.98522700
H	-6.06344200	-1.85391800	9.89052200
H	-4.53046300	-2.39666700	9.20996600
H	-5.86057200	-3.54494000	9.43426300
H	-6.18451500	-0.36558800	6.48404400
H	-6.21282200	-0.03521700	8.21864100
H	-4.71025300	-0.55197300	7.43660200
H	1.39395600	-8.84694300	7.94371400
H	1.00338000	-8.75273800	6.22503300
H	1.10321800	-7.27411800	7.18360300
H	-0.29438800	-8.42420900	9.68918800
H	-1.94969800	-7.94805000	9.31480100
H	-0.61558500	-6.81453600	9.04438900
H	-0.97685700	-10.39970100	6.60844500
H	-0.53275400	-10.47513600	8.31626100
H	-2.18211400	-10.03512500	7.84487400
H	4.76823700	9.89691600	4.54559900

H	7.50075300	9.11316200	1.31534400
H	7.17353400	6.69955500	1.56277800
H	6.23084700	12.66936400	1.08446700
H	6.65127400	11.05354700	0.51263600
H	5.00251300	11.39443200	1.04286100
H	5.79844400	13.14153500	3.46033100
H	5.82683600	11.88964200	4.70103000
H	4.51581000	11.93215600	3.51049500
H	8.56872700	10.95633700	2.27196200
H	8.12201100	12.58417500	2.79225200
H	8.20594400	11.26544000	3.97124100

ANU-2

Total energy: -5114.17123638 a.u.

Charge: 0

Spin: Singlet

Dipole moment: 3.2732 Debye

Function/Basis set: B3LYP/6-311G

N	1.22900000	0.30015800	0.46297900
C	1.01147100	-0.99686100	0.13458600
N	-0.22286400	-1.55753000	0.11251100
C	-1.26630200	-0.75600200	0.43604800
N	-1.12090200	0.54890600	0.77241500
C	0.14078500	1.04424600	0.77664600
C	0.33666700	2.45883900	1.13660100
C	2.16851300	-1.83493800	-0.22041300
C	-2.62375100	-1.32717700	0.41681400

C	-3.73813200	-0.52851900	0.72273700
C	-5.02098700	-1.06581500	0.69576000
C	-5.23394400	-2.41838600	0.36098500
C	-4.11129100	-3.21367500	0.06008900
C	-2.82817500	-2.67873600	0.09007800
C	-0.76247100	3.26909800	1.46639200
C	-0.57853000	4.60635500	1.80251600
C	0.70960000	5.17808200	1.82254800
C	1.80656500	4.35879100	1.49302300
C	1.62380800	3.02298300	1.15267200
C	3.46771500	-1.29821500	-0.22630900
C	4.55808500	-2.08674500	-0.57505800
C	4.39046900	-3.44168200	-0.92220100
C	3.08592400	-3.97598500	-0.90409600
C	1.99314000	-3.18630000	-0.56186200
C	2.13374700	7.73293300	0.19256600
C	3.05421800	8.76002400	-0.08853000
C	3.63819700	8.87368900	-1.34530200
C	3.32247600	7.97446700	-2.38082900
C	2.37566500	6.97037400	-2.10657900
C	1.79759600	6.84563100	-0.84586900
C	-6.63094900	-5.02985600	1.92264400
C	-7.22347800	-6.29804500	2.06719800
C	-6.74501300	-7.20864400	3.00284400
C	-5.66282300	-6.88953000	3.84368900
C	-5.09597900	-5.60778700	3.72151500
C	-5.56216500	-4.69843500	2.77529200

C	7.27996500	-4.09240700	0.63029000
C	8.66912300	-4.05262500	0.85114400
C	9.18655300	-3.66486700	2.08223000
C	8.34097600	-3.31211200	3.15018600
C	6.95228200	-3.39120700	2.93792800
C	6.43016600	-3.76443800	1.70213000
C	0.91093600	6.58919300	2.18437600
C	1.53533200	7.66232600	1.53187400
N	1.51779900	8.79815300	2.32660100
C	0.89002000	8.46493800	3.46005800
N	0.48779700	7.10516300	3.41795700
C	0.59906900	9.22079900	4.61660100
C	-0.04701300	8.62371100	5.67295300
C	-0.41357800	7.24676100	5.60697200
C	-0.14210700	6.50394400	4.49152800
C	-6.58915200	-2.98659800	0.31232800
C	-7.18057400	-4.09894900	0.92858300
N	-8.49008300	-4.25901200	0.50294600
C	-8.73734400	-3.26792200	-0.36108800
N	-7.59004000	-2.44671300	-0.50922700
C	-9.89661800	-2.95103000	-1.10212900
C	-9.88275600	-1.87428700	-1.95664700
C	-8.70239500	-1.08691300	-2.10260600
C	-7.57434700	-1.37905900	-1.38709700
C	5.54740600	-4.26389200	-1.30266900
C	6.78109400	-4.51645700	-0.68428800
N	7.58017700	-5.31514200	-1.48655500

C	6.87385300	-5.57735100	-2.59251900
N	5.60223700	-4.95207600	-2.52439000
C	7.19740100	-6.33081400	-3.74169100
C	6.28884600	-6.42643800	-4.76895700
C	5.03101000	-5.75989600	-4.68033000
C	4.70242600	-5.03124300	-3.57088600
C	8.88779300	-2.92866700	4.48761500
C	8.25192300	-3.62891300	5.64847200
C	9.88985100	-2.01107700	4.64072500
C	10.61463900	-1.81169200	5.93499400
C	10.34786600	-1.12496200	3.52461000
C	3.91349000	8.11290700	-3.74672900
C	5.25090000	8.30081000	-3.96026400
C	2.92453000	8.02952400	-4.86855700
C	5.80776400	8.69700100	-5.29196600
C	6.27393900	8.12282000	-2.88247000
C	-5.17216000	-7.84802700	4.88084800
C	-5.01444000	-7.26297300	6.24999200
C	-4.89445500	-9.15730800	4.60196500
C	-4.66218500	-10.18036000	5.66937000
C	-4.79841700	-9.67994500	3.20265300
C	11.71909500	-0.98182000	3.24196500
C	12.15563700	-0.14542000	2.21381200
C	11.23136300	0.58254400	1.45892200
C	9.86782500	0.46746900	1.74299500
C	9.43088400	-0.37728900	2.76425200
C	10.82922400	-0.51558500	6.44046000

C	11.52254500	-0.31706400	7.63506000
C	12.03445000	-1.40967100	8.34094800
C	11.84706900	-2.70114700	7.84069400
C	11.14457500	-2.90011300	6.65155500
C	7.77329800	-2.91242900	6.76009000
C	7.15605100	-3.57047200	7.82477500
C	7.00485400	-4.95963400	7.80171700
C	7.46594000	-5.68429800	6.69875700
C	8.07383200	-5.02488500	5.62967100
C	1.73527400	8.78111000	-4.83093300
C	0.79966300	8.69406100	-5.86268800
C	1.02404000	7.83892300	-6.94556000
C	2.19153800	7.07196600	-6.98678400
C	3.13175800	7.16699000	-5.95979300
C	7.27015000	9.09502700	-2.67459900
C	8.24014400	8.92739500	-1.68554200
C	8.24743300	7.77422300	-0.89558300
C	7.27674500	6.79070700	-1.10446800
C	6.30078200	6.96315800	-2.08687200
C	6.91809000	8.02144000	-5.83239300
C	7.45440000	8.39512100	-7.06528600
C	6.90451300	9.46592200	-7.77618900
C	5.81560000	10.16002300	-7.24185100
C	5.27322600	9.77974200	-6.01365400
C	-3.83272800	-7.44537700	6.99085600
C	-3.68405000	-6.87289000	8.25481400
C	-4.71428600	-6.10654200	8.80669300

C	-5.89057500	-5.90758800	8.07817700
C	-6.03483800	-6.47144400	6.80982200
C	-3.56417600	-11.05764900	5.59291700
C	-3.35197400	-12.02818300	6.57296100
C	-4.24466000	-12.15610800	7.64108900
C	-5.35068200	-11.30538700	7.71930700
C	-5.55675700	-10.32804200	6.74483000
C	-4.00519300	-9.03499600	2.23648900
C	-3.89567500	-9.54566200	0.94243700
C	-4.57834900	-10.71154700	0.58507900
C	-5.36212100	-11.36962500	1.53725800
C	-5.46254500	-10.86494000	2.83436200
H	-3.57919000	0.50582100	0.98704300
H	-5.86544400	-0.44333300	0.96056000
H	-4.25763100	-4.25237200	-0.20060000
H	-1.97143600	-3.29110300	-0.14642900
H	-1.75151100	2.83750400	1.44315900
H	-1.43869200	5.22383700	2.02532800
H	2.80148000	4.78091200	1.50886100
H	2.46792900	2.39829100	0.90337900
H	3.60200200	-0.25963100	0.03495900
H	5.55104800	-1.66029200	-0.58655900
H	2.93504500	-5.02265400	-1.13280800
H	0.99712000	-3.60187500	-0.54375400
H	3.28869200	9.46777100	0.69260000
H	4.34392600	9.67023200	-1.53386000
H	2.08611300	6.28611400	-2.89257900

H	1.06588600	6.06893100	-0.67967100
H	-8.06887700	-6.54428800	1.44211800
H	-7.21593100	-8.17744300	3.09237800
H	-4.28670300	-5.32134600	4.37964900
H	-5.10740200	-3.72030100	2.71898500
H	9.32656000	-4.34167400	0.04468200
H	10.25754100	-3.63789900	2.22531400
H	6.27769100	-3.16243100	3.75195600
H	5.35841900	-3.82307200	1.58066400
H	0.90404500	10.25561500	4.63146800
H	-0.27524700	9.19204700	6.56304400
H	-0.90749400	6.77450600	6.44269800
H	-0.38477000	5.45934400	4.39039200
H	-10.76417400	-3.57916800	-0.97231300
H	-10.76397700	-1.62164600	-2.52846900
H	-8.68701100	-0.25084500	-2.78537800
H	-6.65282100	-0.82692300	-1.46538900
H	8.16441900	-6.80816500	-3.77434900
H	6.52471500	-7.00110000	-5.65295100
H	4.32423500	-5.82092700	-5.49407100
H	3.77392600	-4.49788100	-3.45556300
H	12.44042300	-1.53302400	3.83021000
H	13.21395000	-0.05980700	2.00436600
H	11.56958700	1.23477700	0.66464800
H	9.14565200	1.03660200	1.17212400
H	8.37497400	-0.46151100	2.97978100
H	10.44757500	0.33542600	5.89254300

H	11.66657600	0.68741600	8.01137200
H	12.57783500	-1.25620700	9.26394600
H	12.24985700	-3.55264200	8.37347000
H	11.00448900	-3.90180100	6.27063100
H	7.88687200	-1.83777300	6.78478900
H	6.79187200	-2.99933500	8.66878500
H	6.52823600	-5.46984600	8.62832700
H	7.34895000	-6.75979800	6.66910100
H	8.41671000	-5.59028100	4.77360300
H	1.54966200	9.43549100	-3.98980600
H	-0.10323500	9.28925800	-5.81975900
H	0.29623200	7.76711300	-7.74303900
H	2.36953900	6.39924400	-7.81560300
H	4.03293700	6.57132100	-5.99821700
H	7.27807600	9.98454500	-3.29015500
H	8.98984100	9.69303500	-1.53390000
H	9.00251900	7.64145200	-0.13210800
H	7.28132700	5.88919600	-0.50568500
H	5.55332700	6.19817500	-2.24431000
H	7.35668400	7.20025200	-5.28158000
H	8.30128400	7.85481500	-7.46800600
H	7.32366100	9.75962600	-8.72950000
H	5.39070500	10.99831800	-7.77836300
H	4.43168200	10.32182100	-5.60610800
H	-3.03171100	-8.03726600	6.57094400
H	-2.76487100	-7.02296100	8.80593400
H	-4.59957600	-5.66503500	9.78787300

H	-6.69233000	-5.31179400	8.49469300
H	-6.94272200	-6.30292300	6.24641800
H	-2.87635800	-10.97303900	4.76228200
H	-2.49474200	-12.68490400	6.50100500
H	-4.08392800	-12.91225700	8.39816000
H	-6.05372200	-11.40374800	8.53613200
H	-6.41505400	-9.67449500	6.81191500
H	-3.47457700	-8.13284500	2.50670700
H	-3.27596900	-9.03634000	0.21586500
H	-4.49573000	-11.10570200	-0.41918400
H	-5.89115000	-12.27557000	1.27148500
H	-6.06081600	-11.38625000	3.56949100

Energy Minimized Structures of ANU-1 and ANU-2 with their dihedral angles

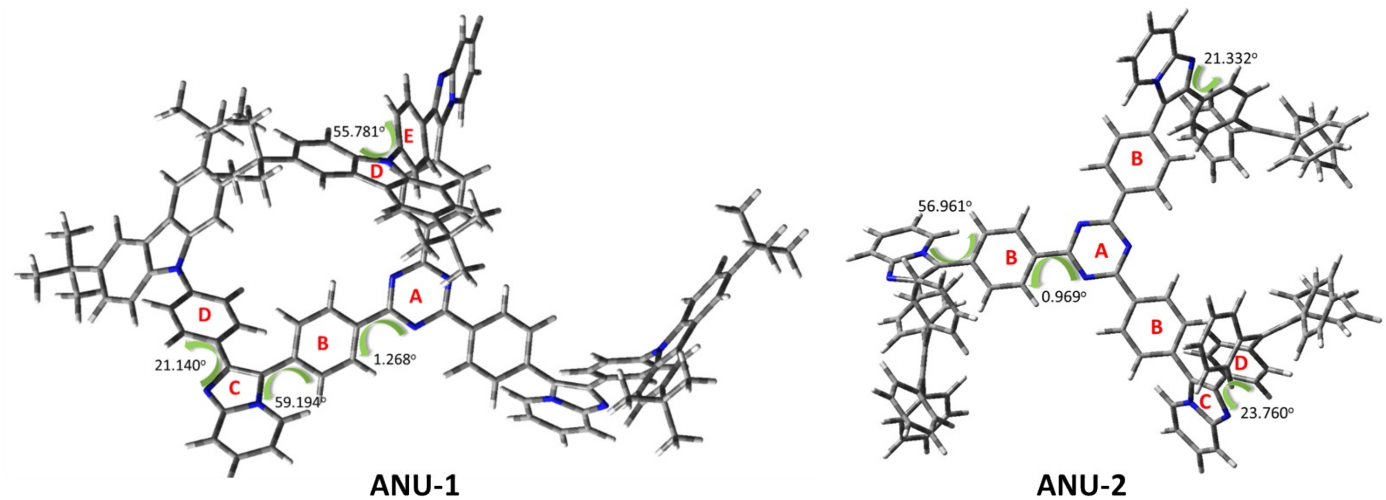

Figure. S6. Energy minimized structure for **ANU-1** and **ANU-2** with their corresponding dihedral angles.

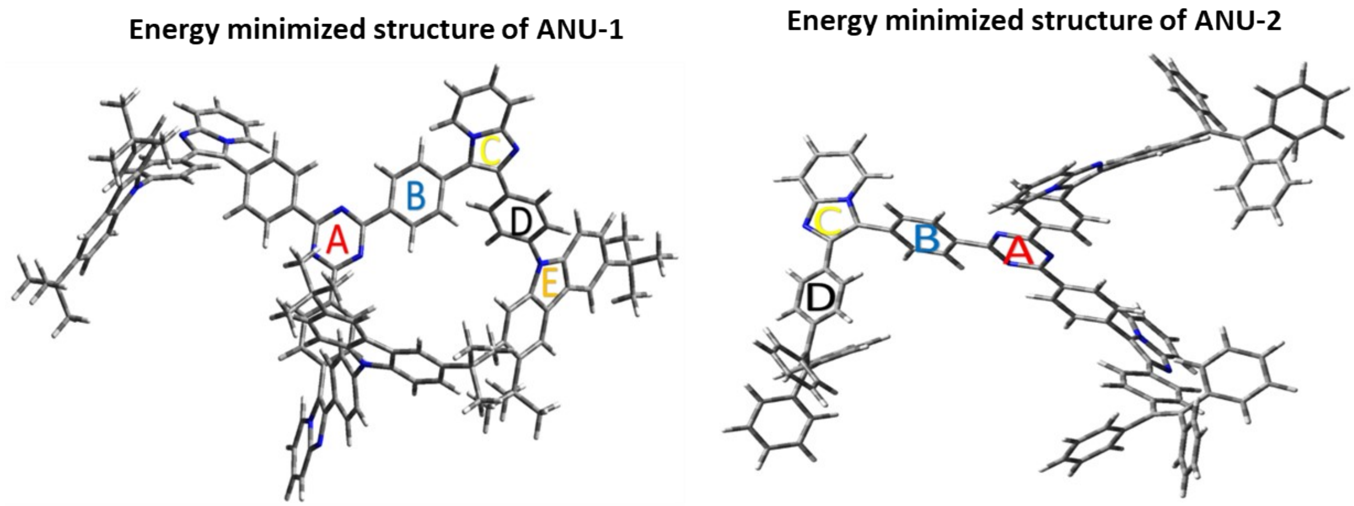

Figure S7. Energy minimized structures of **ANU-1** and **ANU-2**.

Table S3. Dihedral angles existing in **ANU-1 and ANU-2.**

	ANU-1	ANU-2
Dihedral angle between ring A and ring B	1.268 °	0.969°
Dihedral angle between ring B and ring C	59.19 °	56.96 °
Dihedral angle between ring C and ring D	21.14 °	23.76 °
Dihedral angle between ring D and ring E	55.78 °	--

Electrochemical Studies of ANU-1 and ANU-2

Cyclic Voltammetry Analysis of **ANU-1 and ANU-2:** The electrochemical studies including redox potential and theoretical band gap calculations were carried out by cyclic voltammetry studies. The measurements were recorded in an electrolyte solution of 0.1 M tetrabutylammonium hexafluorophosphate ($^{t}Bu_4NPF_6$) in THF using Ag/AgCl as reference electrode and platinum gauze as the counter electrode. Glassy carbon electrode was used as a working electrode and the analysis was carried out at a scan rate of 25 mV/s. The concentration of luminogens (analyte) used was 1 mM. To perform the experiment, the three-electrode system was subjected to a solution containing both analyte and electrolyte in 1:1 proportion.

Bandgap Calculations of ANU-1 and ANU-2

HOMO and LUMO energies and HOMO-LUMO energy gap (EHL) of Luminogens **ANU-1 and ANU-2** calculated at DFT/B3LYP/6-311++ G (d, p) level.

E_{HOMO} = − (4.8 + Eox onset) eV

E_{LUMO} = E_{HOMO} + $E_{band\ gap}$ eV

Band gap = (E_{LUMO} – E_{HOMO}) eV or 1240/ $\lambda_{max\ onset}$

For **ANU-1**

Onset absorption wavelength (λ_{max}) DCM: 395 nm

Onset CV oxidation: 1.182 V

E_{HOMO} = - (4.8 + E_{OX} onset) eV

= - (4.8 + 1.182) eV

= - 5.982 eV

$E_{band\ gap}$ = 1240/λ_{max}

= 1240/395

= 3.13 eV

E_{LUMO} = E_{HOMO} + $E_{band\ gap}$

= - 5.982 + 3.13

= - 2.85 eV

For **ANU-2**

Onset absorption wavelength (λ_{max}) DCM: 406 nm

Onset CV oxidation: 1.189 V

E_{HOMO} = - (4.8 + E_{OX} onset) eV

= - (4.8 + 1.189) eV

= - 5.989 eV

$E_{band\ gap}$ = 1240/λ_{max}

= 1240/406

= 3.05 eV

E_{LUMO} = E_{HOMO} + $E_{band\ gap}$

= -5.989 + 3.05

= - 2.939 eV

Temperature Dependant Fluoroscence Decay Lifetimes for ANU-1 and ANU-2:

Table S4: Temperature Dependant Fluoroscence Decay Lifetime for **ANU-1** in thin film:

ANU-1	τ_1 (ns)	τ_2 (ns)	B1	B2	Average Time (ns)
77K	1.855	6.191	120.242	111.467	3.941
100K	2.077	6.546	136.690	109.184	4.061
150K	1.816	6.365	120.018	110.870	4.009
200K	1.809	6.746	146.018	131.568	4.149
250K	1.668	7.401	174.328	117.729	3.979
300K	1.603	6.949	257.994	139.755	3.481

Table S5: Temperature Dependant Fluoroscence Decay Lifetime for **ANU-2** in thin film

ANU-2	τ_1 (ns)	τ_2 (ns)	B1	B2	Average Time (ns)
77K	1.924	4.336	228.872	192.139	3.025
100K	2.057	4.540	256.214	162.891	3.022
150K	1.945	4.737	268.591	143.943	2.919
200K	1.701	4.485	250.313	159.977	2.786
250K	1.517	4.318	247.491	166.590	2.644
300K	1.230	3.785	262.076	150.684	2.163

Picric Acid Sensing Studies of ANU-1 and ANU-2

The fluorescence sensing ability of the synthesized luminogen toward picric acid (TNP) was investigated due to its electron-deficient nature and strong quenching ability. The interaction with TNP was monitored through changes in fluorescence intensity upon incremental addition in organic solvent (THF) and aqueous medium (aggregated state for ANU-2). Nitroaromatic used for the study were trinitrophenol, 1-nitronapthalene, *p*-nitrobenzaldehyde, *p*-nitrobenzoic acid, *p*-nitrophenol, *p*-nitrobenzylbromide, *p*-nitroacetophenone and *p*-nitrotoluene.

For selectivity experiment 1 mM stock solution was made of each nitroaromatic and equal volume of it was added to the emissive luminogen solution. Emission was recorded of each nitroaromatic with the help of a spectrofluorimeter.

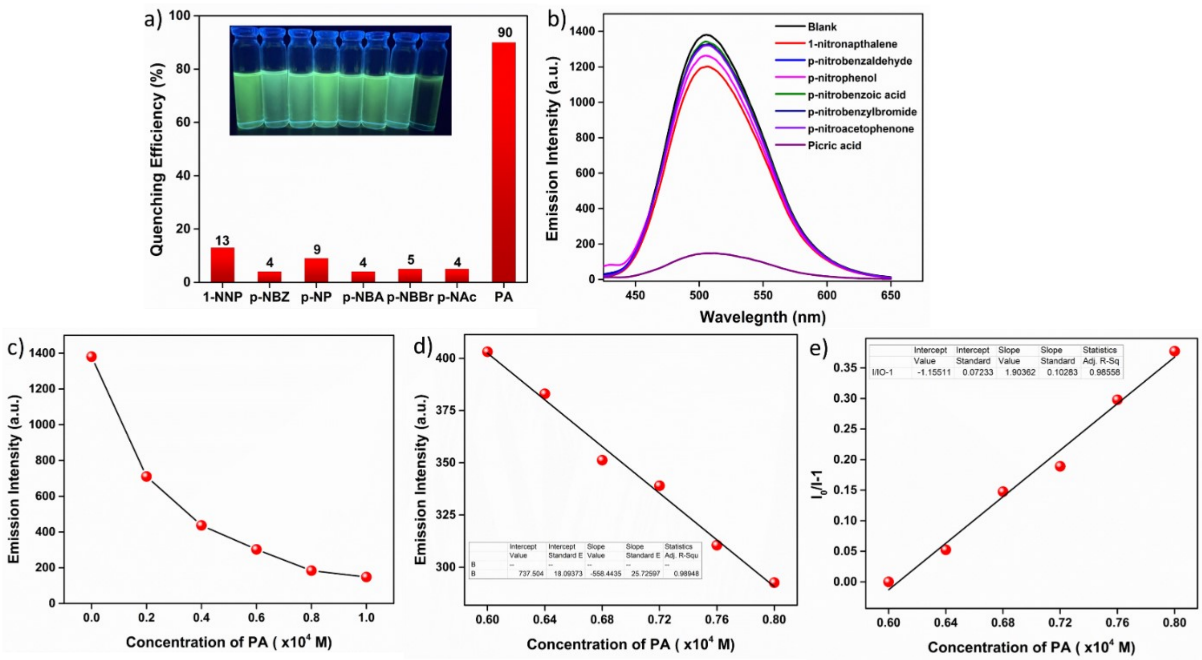

Figure S8. a) Quenching efficiency of **ANU-1** in THF with all the nitroaromatics, b) Emission spectra of **ANU-1** in THF with nitroaromatics, c) Plot of emission intensity of **ANU-1** in THF versus gradual increase in concentration of picric acid for detection limit calculation, d) Graphical plot for the calculation of LoD of picric acid **ANU-1** in THF, e) Quenching constant calculation graph.

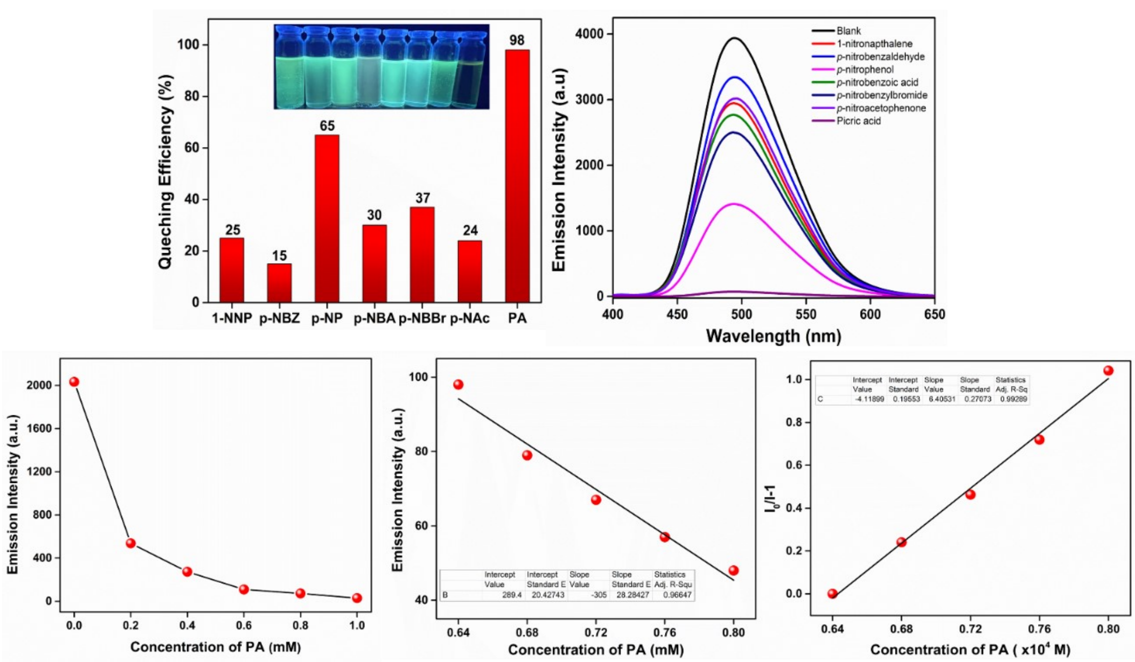

Figure S9. a) Quenching efficiency of **ANU-2** in aggregated state with all the nitroaromatics, b) Emission spectra of **ANU-2** in aggregated state (70:30 Water:THF) with nitroaromatics, c) Plot of emission intensity of **ANU-2** in aggregated state (70:30 Water:THF) versus gradual increase in concentration of picric acid for detection limit calculation, d) Graphical plot for the calculation of LoD of picric acid by **ANU-2** in aggregated state (70:30 Water:THF), e) Quenching constant calculation graph.

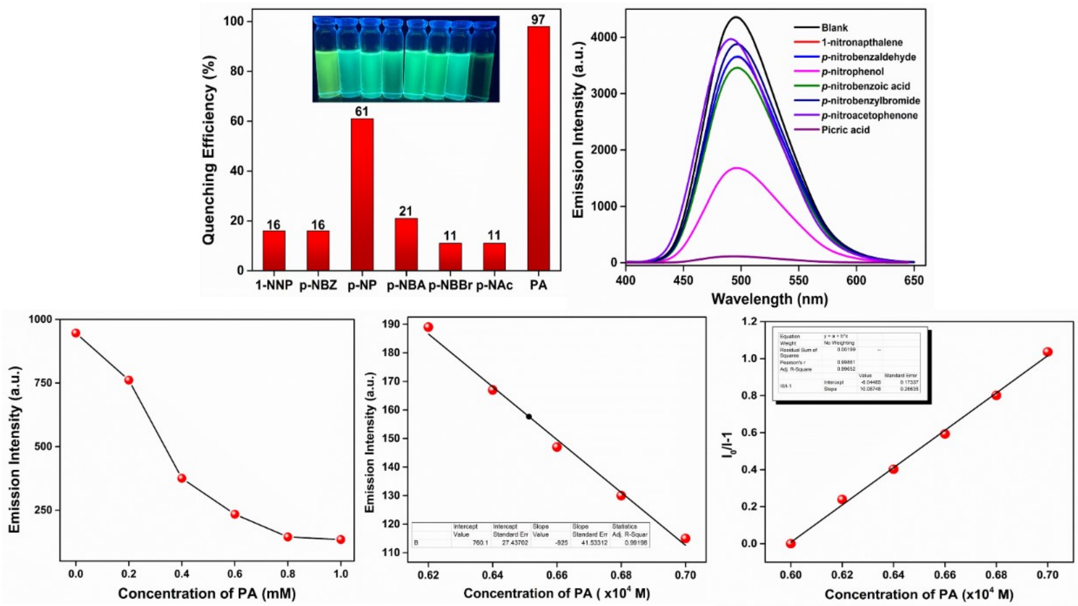

Figure S10. a) Quenching efficiency of **ANU-2** in THF with all the nitroaromatics, b) Emission spectra of **ANU-2** in THF with nitroaromatics, c) Plot of emission intensity of **ANU-2** in THF versus gradual increase in concentration of picric acid for detection limit calculation, d) Graphical plot for the calculation of LoD of picric acid by **ANU-2** in THF, e) Quenching constant calculation graph.

- Detection limit calculations for **ANU-1** (1 mM) in THF with PA

σ = Standard Deviation obtained from 7 blank emission measurement of THF

σ = **26.12**

and k is slope obtained from Plot of emission intensity of **ANU-1** in THF versus concentration of PA (0.6 mM to 0.8 mM) in THF

k = **558.443**

Detection limit = 3σ/k

Detection limit = 3*26.12/558.443

Detection limit = **0.140 mM** = **32.07 ppm**

Quenching Constant (K_{sv}) = **1.903*10⁴ M⁻¹** obtained from slope of concentration of picric acid (0.6 mM to 0.8 mM) versus I_0/I-1 where I_0 is the maximum emission value at 0.6 mM.

- Detection limit calculations for **ANU-2** in aggregated state (70:30 Water:THF) with PA

σ = Standard Deviation obtained from 7 blank emission measurement of aggregated state (70:30 Water:THF)

σ = **79.948**

and k is slope obtained from Plot of emission intensity of **ANU-2** in aggregated state (70:30 Water:THF) versus concentration of PA (0.64 mM to 0.8 mM) in THF

k = **305**

Detection limit = 3σ/k

Detection limit = 3*79.948/305

Detection limit = **0.786 mM** = **180.07 ppm**

Quenching Constant (K_{sv}) = **6.40*10⁴ M⁻¹** obtained from slope of concentration of picric acid (0.64 mM to 0.80 mM) versus $I_0/I-1$ where I_0 is the maximum emission value at 0.64 mM.

- Detection limit calculations for **ANU-2** in THF with PA

σ = Standard Deviation obtained from 7 blank emission measurement of THF

σ = **49.762**

and k is slope obtained from Plot of emission intensity of **ANU-2** THF versus concentration of PA (0.62 mM to 0.7 mM) in THF

k = **925**

Detection limit = 3σ/k

Detection limit = 3*49.762/925

Detection limit = **0.161 mM** = **36.88 ppm**

Quenching Constant (K_{sv}) = **10.087*10^4 M^{-1}** obtained from slope of concentration of picric acid (0.6 mM to 0.7 mM) versus $I_0/I-1$ where I_0 is the maximum emission value at 0.6 M.

Comparison of the HOMO-LUMO energy band gap between the luminogens ANU-1, ANU-2 and TNP

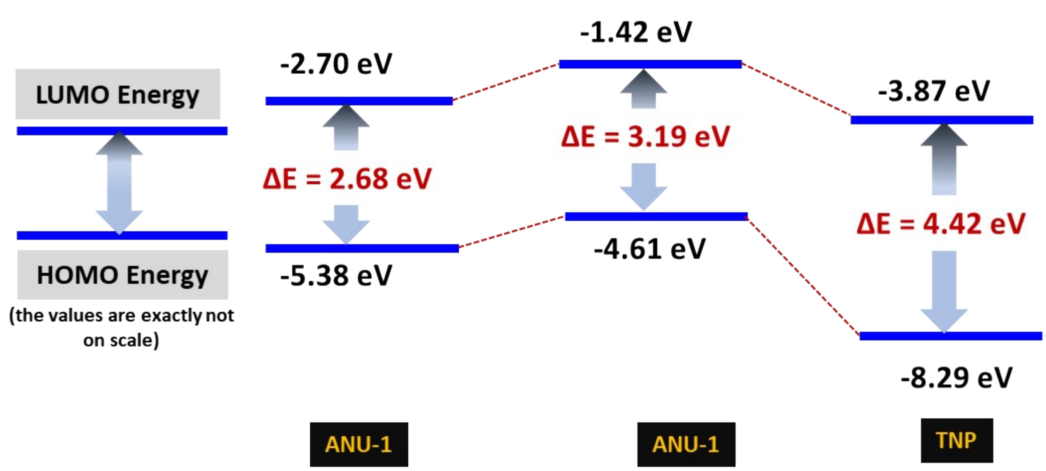

Figure S11. The experimentally calculated HOMO-LUMO band gap of the luminogens, **ANU-1**, **ANU-2** and TNP.

Table S6. Literature reported luminogens and their corresponding LOD values for the detection of TNP.

Sr. No	Compound	LOD Value	Reference
1	BBHN	4.04 µM	Spectrochim. Acta A Mol. Biomol. Spectrosc. 2024, 305, 123465
2	TPA-1	4.7 µM	Sci. Rep. 2021, 11, 19324
3	MP	39 µM	ChemistrySelect 2021, 6, 12300-12308
4	3c	19 µM	ChemistrySelect, 2018, 3, 4598-4608
5	2′-benzyloxy flavone	4 nM	Sens. Diagn., 2024, 3, 1263–1271
6	$Eu(L)(NO_3)_3(H_2O)$	0.38 µM	ChemistrySelect, 2016, 1, 1943–1948
7	TPE-DMA	4.088 µM	ChemistrySelect 2023, 8, e202204354
8	T1, T2	1.94 nM, 2.24 nM	J. Photochem. Photobiol. A Chem. 429 (2022) 113921.
9	TZNET	203 nM	Ind. Eng. Chem. Res. 60 (2021) 7987–7997
10	TRZDPA	0.37 nM	Mater. Today Chem. 12 (2019) 178–186
11	NPhDCzT	65 nM	Chem. Eur. J. 18 (2012) 15655–15661
12	TPEH, TPEOMe, TPEtBu, TPEOH, TPECN, TPEPy	1.64 µM, 0.5µM, 0.93µM, 1.48µM, 0.49µM, 0.35µM	Dyes and Pigments 220 (2023) 111743
13	M1, M2, M3	203 nM, 198 nM, 363 nM	CrystEngComm, 2022, 24, 6865–6872
14	TL18	99 nM	Anal. Chem. 2019, 91, 13244–13250
15	TPEBF	497 nM	Anal. Methods, 2021, 13, 2830–2835
16	TPEcTPE, TPEcTPa, TPAcTPE	0.68 µM, 0.64 µM, 0.32 µM	J. Mater. Chem. C, 2022, 10, 6078–6084
17	CzIP	3 nM	Materials Today Chemistry 30 (2023) 101548
18	Probe 5	0.119 µM	Ind. Eng. Chem. Res. 2024, 63, 23, 10077–10092
19	DCDHF	27 nM	ChemPhysChem 2024, 25, e202400264
20	L	0.0017 mM	RSC Adv., 2015, 5, 191–195
21	Probe A	0.01 µM	Tetrahedron Lett., 2015, 56, 7094-7099
22	IMPY	0.21 µM	*Sens. Actuators, B*, 2017, **245**, 665-673.
23	Probe	23.2 nM	*RSC Adv.*, 2016,**6**, 38328-38331
24	Probe	1.5 µM	*Anal. Chim. Acta*, 2015, **864**, 55-63.
25	Probe 1	0.25 µM	*Chem. Commun.*, 2017,**53**, 10524-10527
26	C1 and C2	4.21 nM and 11.61 nM	Sens. Actuators B Chem. 2016, 234, 34-45
27	CZCS	0.119 µM	ChemPhotoChem 2022, 6, e202200184
28	M1 and M2	4.7 µM and 6.0 µM	CrystEngComm, 2018, 20, 1237–1244
29	Sensor 1 and Sensor 2	1.99 µM and 1.51 µM	J. Org. Chem. 2013, 78, 3, 1306–1310

Cell Imaging studies of ANU-1 and ANU-2

Biocompatibility and cytotoxicity assay

The colorimetric 3-(4,5-dimethylthiazol-2-yl)-2,5-diphenyl tetrazolium bromide (MTT) assay was carried out to check the cell viability/toxicity. HEK-293 (human embryonic kidney cell lines) and HeLa cells were used to analyze the cell viability and cytotoxicity assay, respectively. The cells were cultured in complete DMEM and were harvested by trypsinization for seeding in the well plate. Briefly, the cellular suspension of ~12,000-14,000 cells/well was seeded in a 96-well plate. Then, the cells were incubated for 24 hours to facilitate the cellular attachment on the surface of the well at 37 °C with 5% CO_2. After one wash with sterile phosphate buffer, different concentrations (0.1 to 25 µg/ml) of ANU-1 and ANU-2 were added into the wells in a triplicate manner. For positive control, 0.5% Triton X-100, and for growth/negative control, complete DMEM media were used. After 24 hours of treatment with the luminogens, the samples were removed, and two gentle PBS washes were given to the cells to remove the test samples properly. MTT solution (50 µg/well) was added to each well and further incubated for 2 hours (facilitates the conversion of MTT to formazan). Afterward, DMSO was added to each well to dissolve formazan. The formazan's optical density (OD) was then measured at 570 nm using a plate reader (Tecan Infinite M200 Pro). Cellular viability was calculated for the wells treated with AIEgens depending on the OD data. The percentage cell viability was calculated using the following equation:

% Cell viability = {(Absorbance of test sample-Absorbance of media control)/(Absorbance of growth control- Absorbance of media control)}*100

***In-vitro* ROS detection assay**

The intracellular ROS levels in HEK-293 and HeLa cells were evaluated using the fluorescent probe DCFDA. Different concentrations (0.1 to 25 µg/ml) of ANU-1 & ANU-2 were added to HEK-293 cell cultures; however, only at a 1 µg/ml concentration were they added to the HeLa cells seeded separately in the 96-well plates. This study considers cells without any treatment as a growth or negative control and 10 µM H2O2-treated cells as a positive control. The 10 µM H_2O_2 was added just 2 hours before the addition of the DCFDA probe. After 24-hour incubation, the ANU-1 and ANU-2 were removed from the cells, followed by PBS washing. Thereafter, 10 µM DCFDA was added to all the treated wells and incubated in the dark for 45 minutes. After removing DCFDA, the cells were washed twice with serum-free media, followed by PBS. The ROS-induced green fluorescence generation was measured immediately using the microplate reader (at 485 nm excitation and 535 nm emission).

***In-vitro* cellular uptake**

HeLa cells were used to analyze the fluorescent behaviour of the compound inside the cells. The cells were seeded on the sterile coverslips in a 12-well plate at a cell density of ~50,000 cells/well and incubated for 24 hours. Then, ANU-1 and ANU-2 were added to the wells at a 1 µg/ml concentration, and the cells were incubated again for 24 hours. In growth control, the cells were treated with the complete media. Following the removal of ANU-1 and ANU-2 from the wells, PBS washes were given to the cells twice the next day. The cells were then incubated for 15 minutes with 4% formaldehyde to fix them. Afterward, three PBS washes were given to remove formaldehyde. The nuclear staining was done using 2 µg/ml DAPI. Three consecutive PBS washes were given after the staining with DAPI. The coverslips were further fixed on a glass slide, and cells were then viewed by 63X confocal laser scanning microscopy (CLSM).

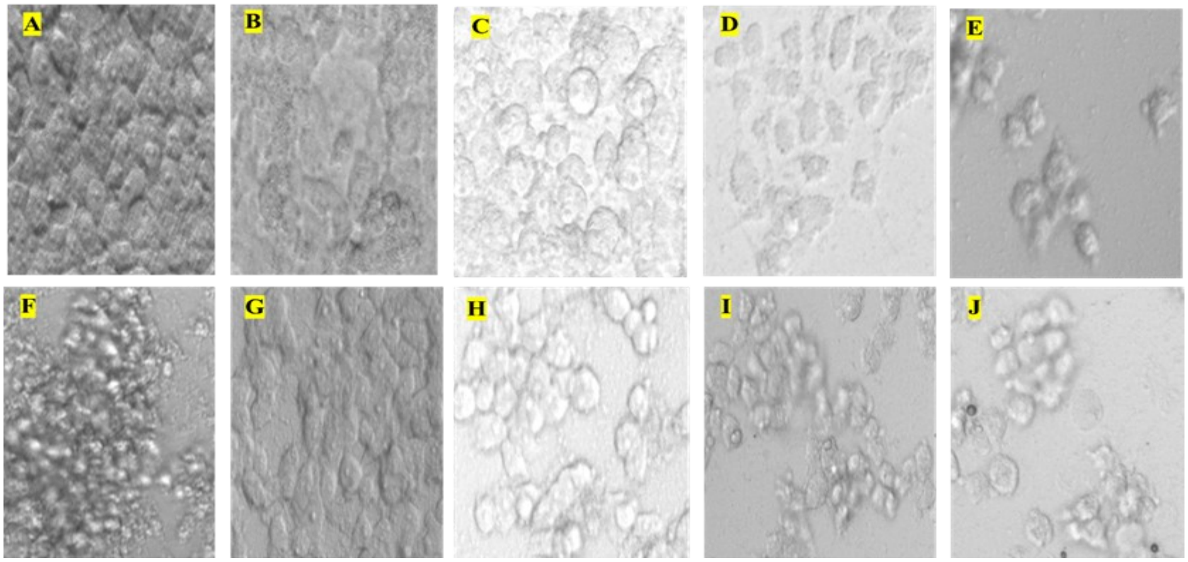

Figure S12. Two-dimensional images representing concentration-dependent inhibition of HEK-293 cell growth after 24-hour incubation with luminogens. A and F show growth control and positive control, respectively. B to E depicting the morphology of cells treated with 0.1, 1, 10, 25 µg/ml of **ANU-1.** G to J depicting the morphology of cells treated with 0.1, 1, 10, 25 µg/ml of **ANU-2.**

Reactive Oxygen Species Experimental Details for ANU-1 and ANU-2.

A 1 mM stock solution of DCFH-DA was prepared in dry ethanol. For the assay, 3 mL of dry ethanol was transferred into a quartz cuvette, and 120 µL of the DCFH-DA stock solution was added, resulting in a final concentration of 40 µM. Subsequently, 120 µL of 40 µM NaOH solution was added, and the mixture was ultrasonicated in the dark for 15 minutes to hydrolyze DCFH-DA to DCFH-OH, the non-fluorescent ROS-sensitive intermediate.

Following this, 60 µL of luminogen solution (**ANU-1** or **ANU-2**, 40 µM) was added to the cuvette. The solution was mixed thoroughly, kept protected from light, and then exposed to white light. Fluorescence measurements were recorded at 2-minute intervals, using an excitation wavelength of 504 nm and monitoring emission at 530 nm, corresponding to the oxidized fluorescent form DCF.

A blank control (without luminogen) was prepared and analyzed under identical conditions. In the absence of luminogen, the DCFH-OH solution showed only a marginal increase in fluorescence intensity over a 40-minute period, indicating minimal ROS generation. In contrast, solutions containing **ANU-1** and **ANU-2** showed a significant enhancement in fluorescence intensity on white light irradiation, as presented in Figure S13.

These results clearly demonstrate that luminogens **ANU-1** and **ANU-2** actively generate reactive oxygen species (ROS) upon photoexcitation, as evidenced by the strong increase in DCF fluorescence under light exposure.

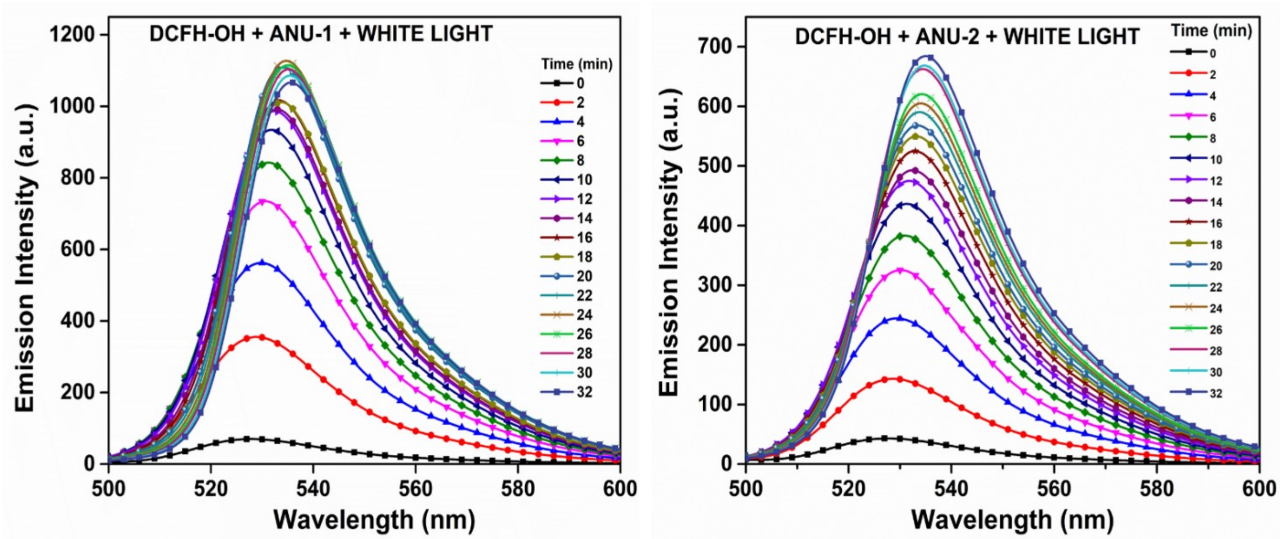

Figure. S13. Fluorescence emission spectra of **ANU-1** and **ANU-2** in presence of DCFH-DA after subjecting to white light at every 2 min interval.

^{1}H and ^{13}C NMR Spectral Representations of 10, ANU-1 and ANU-2

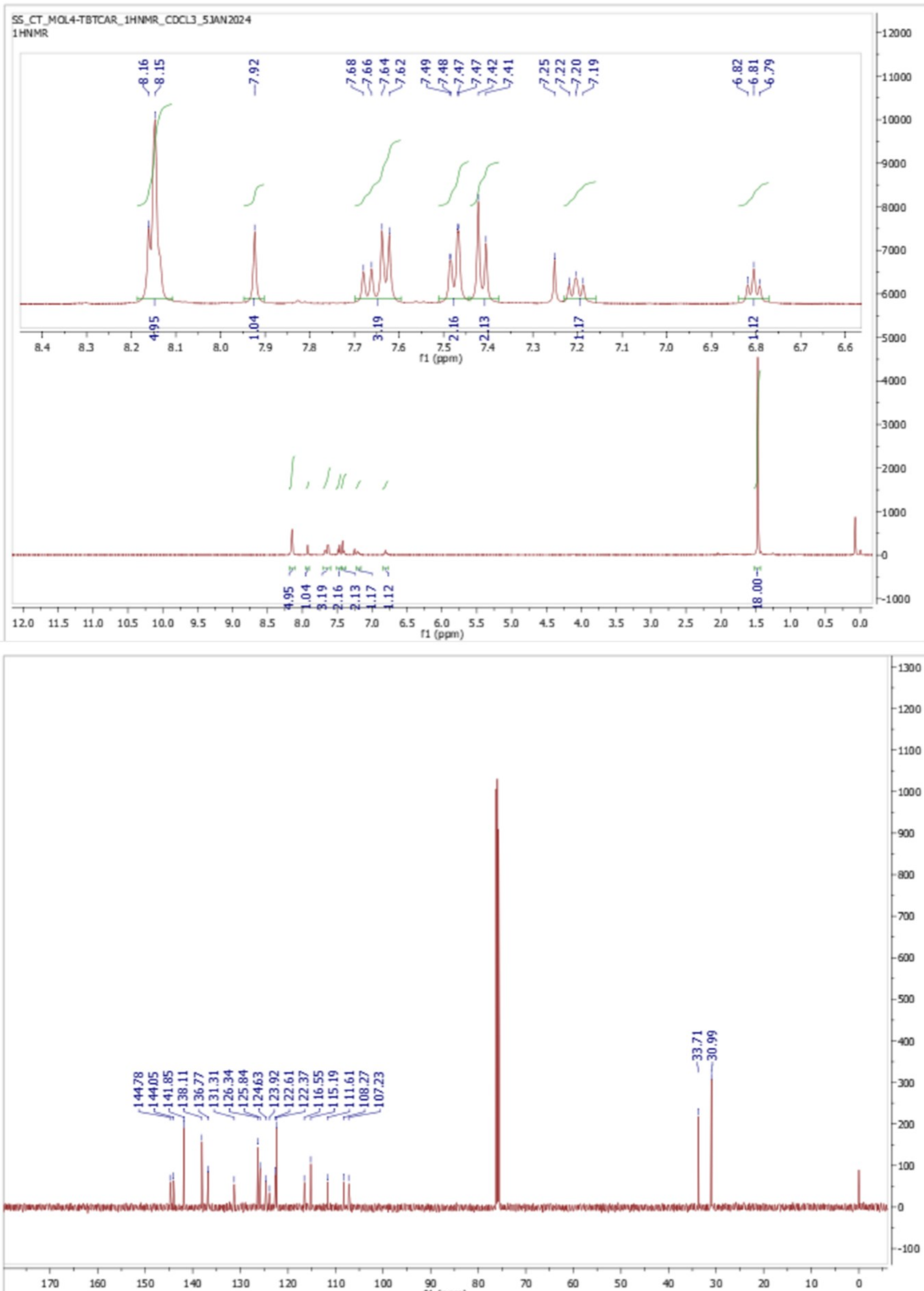

Figure. S14. ^{1}H NMR (500 MHz, $CDCl_3$) and ^{13}C NMR (126 MHz, $CDCl_3$) spectra of 3,6-di-tert-butyl-9-(4-(imidazo[1,2-a]pyridin-2-yl)phenyl)-9H-carbazole **10.**

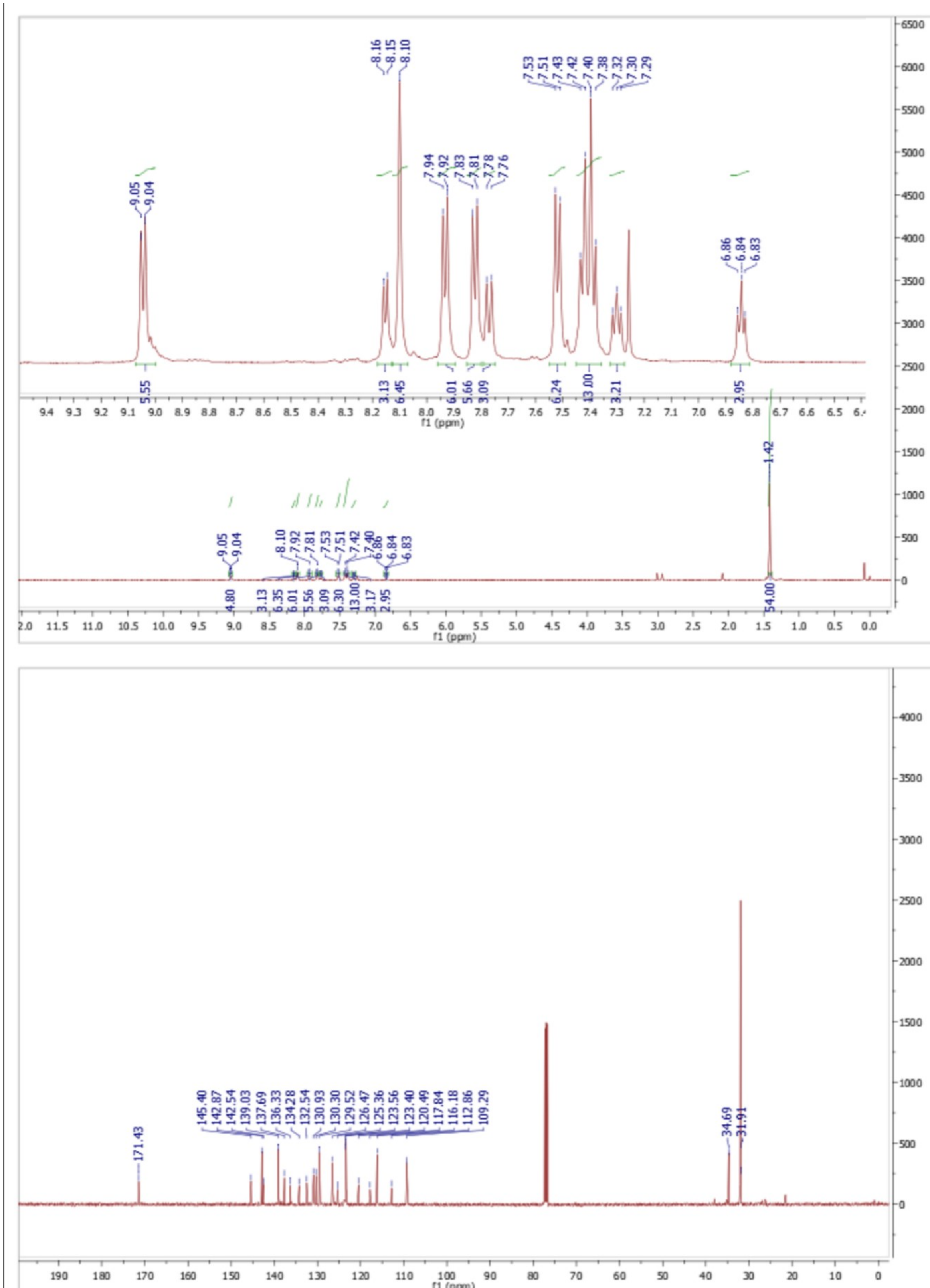

Figure. S15. ^1H NMR (500 MHz, $CDCl_3$) and ^{13}C NMR (126 MHz, $CDCl_3$) spectra of 2,4,6-tris(4-(2-(4-(3,6-di-tert-butyl-9H-carbazol-9-yl)phenyl)imidazo[1,2-a]pyridin-3-yl)phenyl)-1,3,5-triazine **ANU-1.**

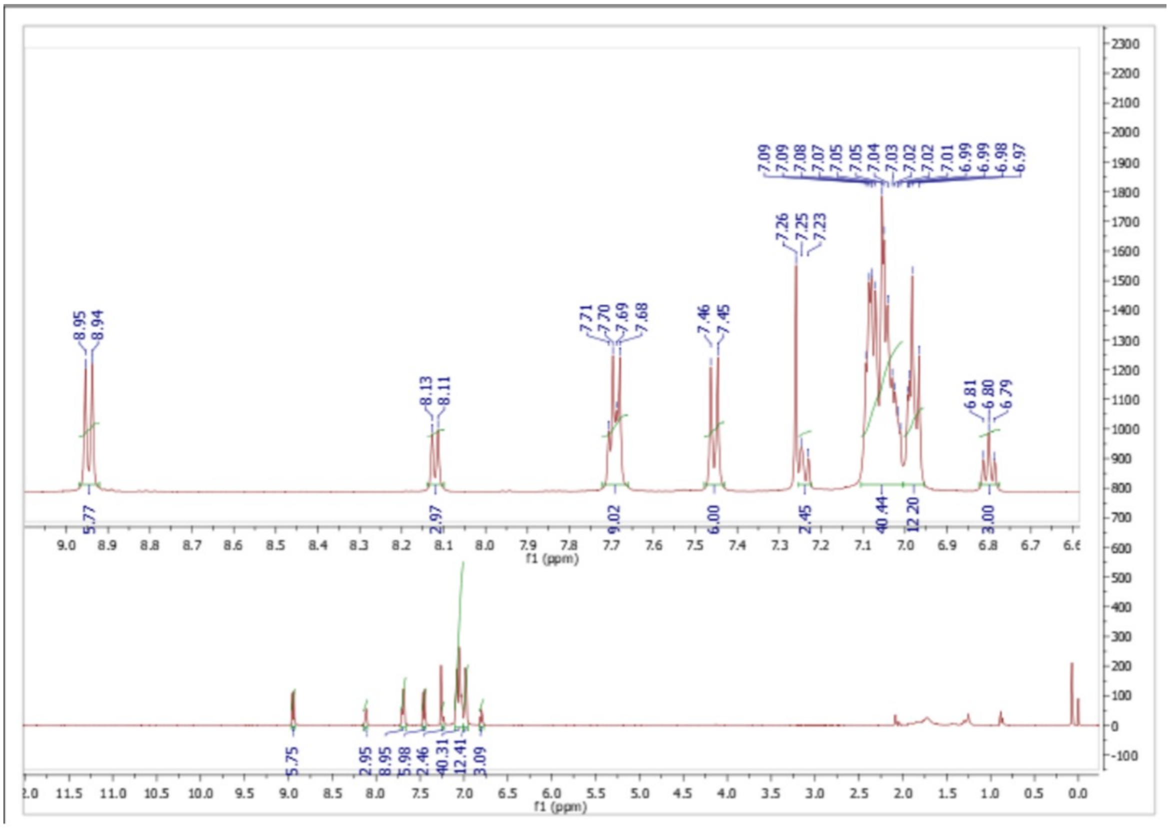

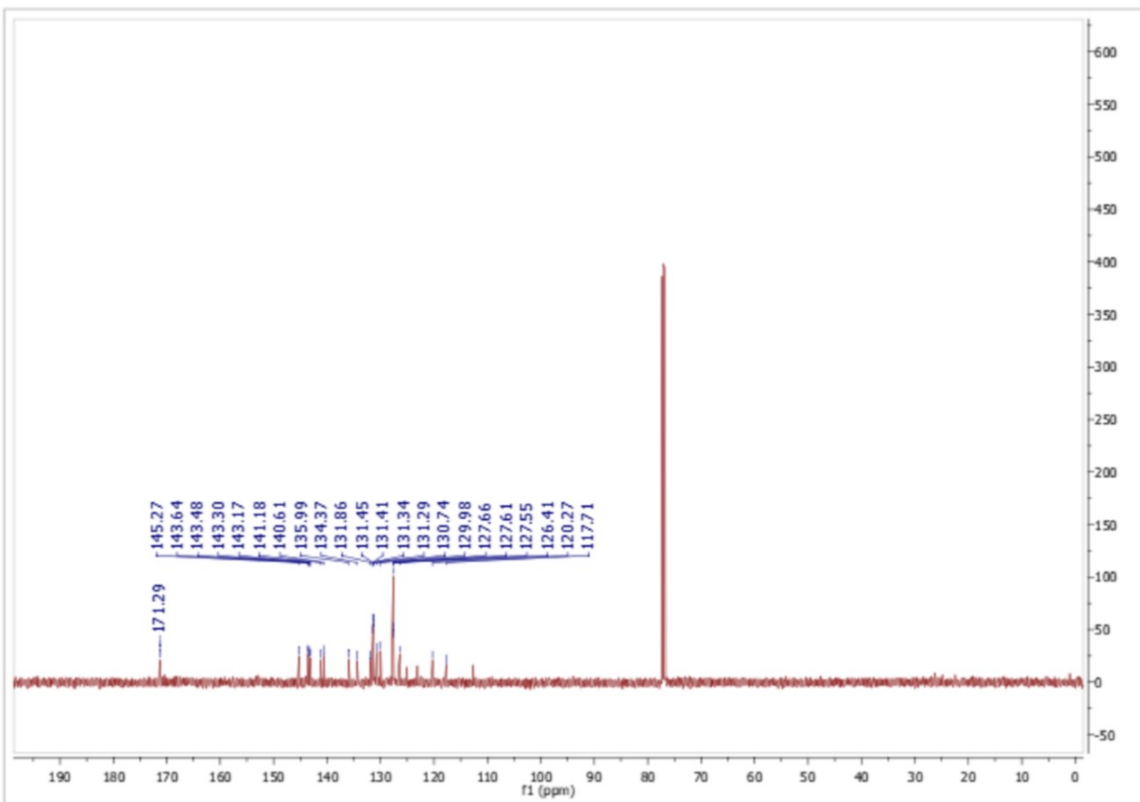

Figure. S16. ^{1}H NMR (500 MHz, $CDCl_3$) and ^{13}C NMR (126 MHz, $CDCl_3$) spectra of 2,4,6-tris(4-(2-(4-(1,2,2-triphenylvinyl)phenyl)imidazo[1,2-a]pyridin-3-yl)phenyl)-1,3,5-triazine **ANU-2.**

LC-HRMS Data of ANU-1 and ANU-2.

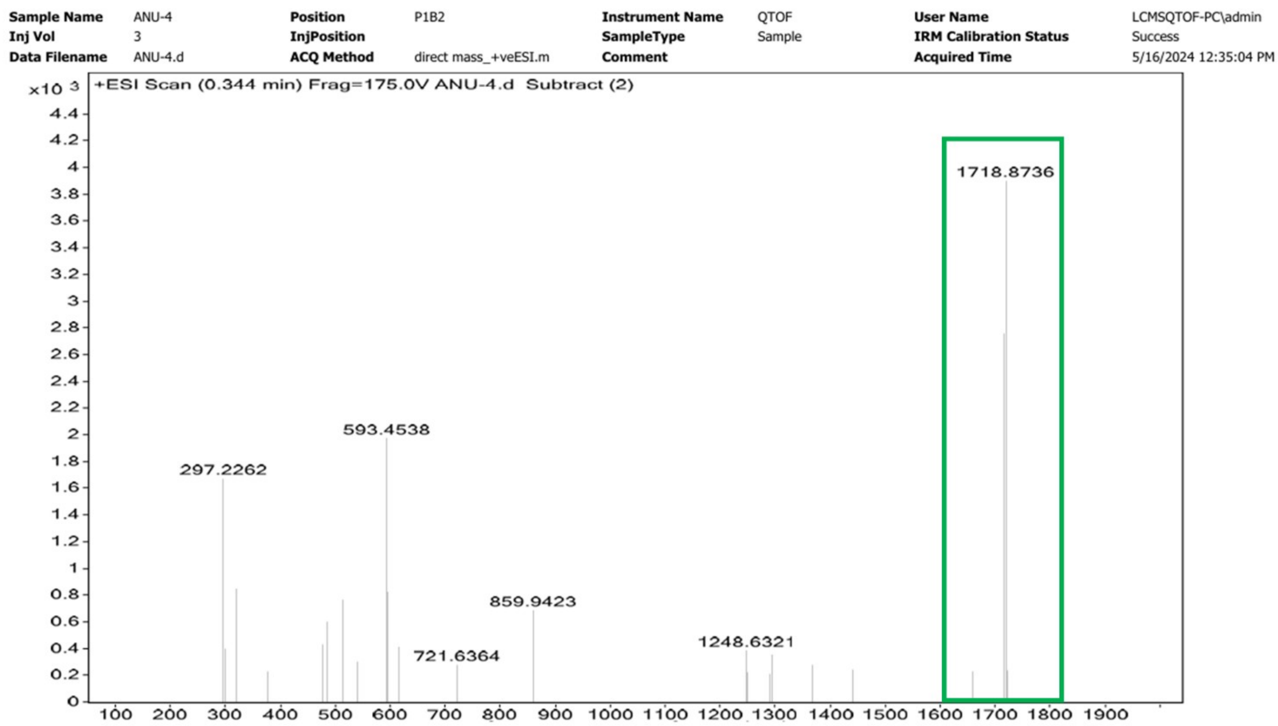

Figure. S17. LC-HRMS spectra of 2,4,6-tris(4-(2-(4-(3,6-di-tert-butyl-9H-carbazol-9-yl)phenyl)imidazo[1,2-a]pyridin-3-yl)phenyl)-1,3,5-triazine **ANU-1.**

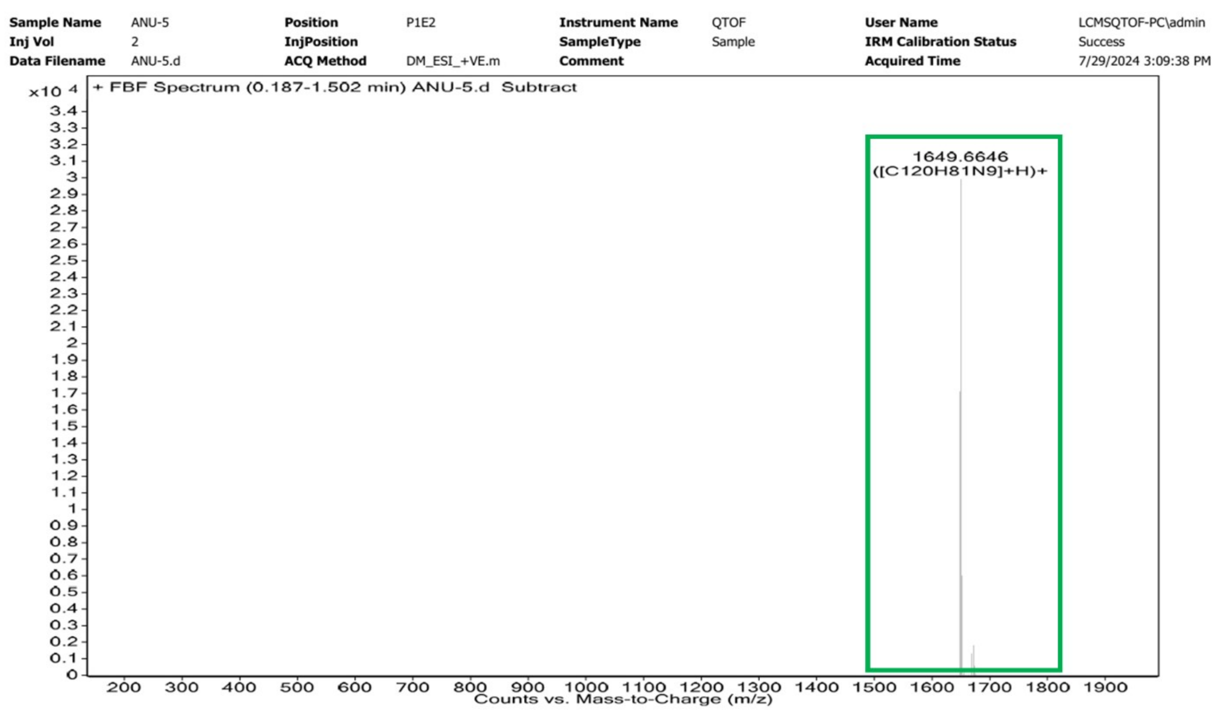

Figure. S18. LC-HRMS spectra of 2,4,6-tris(4-(2-(4-(1,2,2-triphenylvinyl)phenyl)imidazo[1,2-a]pyridin-3-yl)phenyl)-1,3,5-triazine **ANU-2.**

References.

1. K. Barman, A. K. Sharma, S. Bhowmick and P. K. Iyer, *Chem. Eur. J.*, 2025, **31**, e202500047.
2. C. Thakkar, S. Kale, M. A. Ahemad, M. Debnath, A. Tripathi, S. Seth, P. Badani, R. Srivastava, S. Bose and S. Saha, *J. Mater. Chem. C*, 2025, **13**, 10576–10591.
3. (a) M. Arshad, M. S. Alqahtani, S. K. Alanazi, M. S. M. Abdelbaky, A. Joseph and S. M. A. Pike, *Spectrochim. Acta, Part A*, 2024, **305**, 123465; (b) A. Mishra, R. Dheepika, P. A. Parvathy, P. M. Imran, N. S. P. Bhuvanesh and S. Nagarajan, *Sci. Rep.*, 2021, **11**, 19324; (c) A. Shabashini, M. Karthikeyan, M. K. Panda and G. C. Nandi, *Chem. Select*, 2021, **6**, 12300–12308; (d) S. Chaudhary, H. Sharma and M. D. Milton, *Chem. Select*, 2018, **3**, 4598–4608; (e) P. Bhardwaj, A. Kumar and H. B. Kraatz, *Sens. Diagn.*, 2024, **3**, 1263–1271; (f) A. K. Unnava and A. Saikia, *Chem. Select*, 2016, **1**, 1943–1948; (g) H. A. Mirgane, N. Gosavi and K. S. More, *Chem. Select*, 2023, **8**, e202204354; (h) S. Farooq, S. A. Shahzad, M. A. Rauf, A. Mahmood, K. Ayub and R. A. Khera, *J. Photochem. Photobiol., A*, 2022, **429**, 113921; (i) H. Muniyasamy, C. Chinnadurai, M. Nelson, A. Veeramanoharan and V. Ashokkumar, *Ind. Eng. Chem. Res.*, 2021, **60**, 7987–7997; (j) P. S. Mahajan, G. D. Sharma and K. R. Justin Thomas, *Mater. Today Chem.*, 2019, **12**, 178–186; (k) J. Chen, J. Yin, J. J. Xiao, H. F. Shi, Y. Tao, Y. Qian and W. Huang, *Chem. Eur. J.*, 2012, **18**, 15655–15661; (l) L. Wang, S. Yang, W. Fan, X. Wang, Y. Kou and H. Tan, *Dyes Pigm.*, 2023, **220**, 111743; (m) Y. Zhang, F. Tang, A. Ding, F. He, J. Huang and L. Yuan, *CrystEngComm*, 2022, **24**, 6865–6872; (n) A. Kathiravan, A. Gowri, T. Khamrang, M. D. Kumar and N. Dhenadhayalan, *Anal. Chem.*, 2019, **91**, 13244–13250; (o) Y. Ni, S. Zhang, X. He, J. Huang, L. Kong, J. Yang and J. Yang, *Anal. Methods*, 2021, **13**, 2830–2835; (p) Y. Zhang, A. Ding, S. Guo, F. He, L. Kong, R.-H. Duan and J. Yang, *J. Mater. Chem. C*, 2022, **10**, 6078–6084; (q) J. Jiang, C. Hu, Y. Wang, L. Zhang, X. Chen, J. Liu and H. Zhang, *Mater. Today Chem.*, 2023, **30**, 101548; (r) R. Rai, R. Bhandari, M. Kaleem, N. Shraogi and S. Sindhu, *Ind. Eng. Chem. Res.*, 2024, **63**, 10077–10092; (s) K. S. Chakkumkumarath and L. C., *ChemPhysChem*, 2024, **25**, e202400264; (t) Y. Li, X. Hao and J. Qi, *RSC Adv.*, 2015, **5**, 191–195; (u) G. A. Ardizzoia, S. Brenna, S. Durini and B. Therrien, *Tetrahedron Lett.*, 2015, **56**, 7094–7099; (v) R. Sodkhomkhum, D. Dhara, C. S. P. Tripathy, A. Ervithayasuporn and S. T. I. Mahmud, *Sens. Actuators, B*, 2017, **245**, 665–673; (w) S. Areti, V. P. Yadav, S. K. Mishra and A. Kumar, *RSC Adv.*, 2016, **6**, 38328–38331; (x) S. Shanmugaraju, C. D. S. Fraser, A. Neale, M. A. Kitchen, T. J. Gray, M. E. Nimick, R. H. Plummer and P. B. Crowley, *Anal. Chim. Acta*, 2015, **864**, 55–63; (y) Y. Peng, A.-Y. Zhang, M. Dong and Y. Wang, *Chem. Commun.*, 2017, **53**, 10524–10527; (z) K. Ponnuvel, G. Banuppriya and V. Padmini, *Sens. Actuators, B, Chem.*, 2016, **234**, 34–45; (aa) Y. Zhang, X. Li, J. Wang, Z. Li, Y. Liu and J. Yin, *ChemPhotoChem*, 2022, **6**, e202200184; (ab) J. Yang, Y. Guo, A. Ding, F. He, L. Kong, R.-H. Duan and S. Zhang, *CrystEngComm*, 2018, **20**, 1237–1244; (ac) R. Guo, T. Jiao, R. Li, Y. Chen, W. Guo, L. Zhang, J. Zhou, Q. Zhang, Q. Peng and S. Yan, *J. Org. Chem.*, 2013, **78**, 1306–1310.